Magnetic Helicoidal Dichroism (MHD)

Mauro Fanciulli

CY Cergy Paris University, DICO LIDYL - CEA Saclay, France

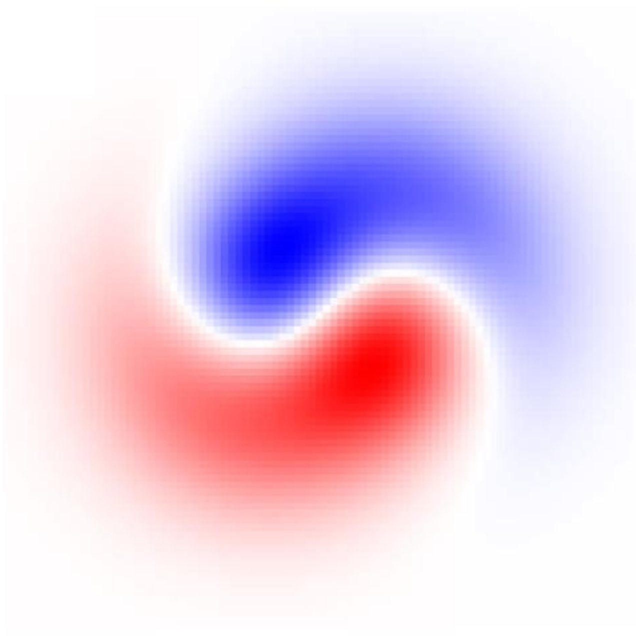

陰
陽

SPICE - Characterization and control of quantum materials with optical vortex beams

Ingelheim, 11/06/2025

Magnetic ~~Helicoidal~~ Dichroism (MHD)
Magnetic Vortex Dichroism (MVD)

Mauro Fanciulli

CY Cergy Paris University, DICO LIDYL - CEA Saclay, France

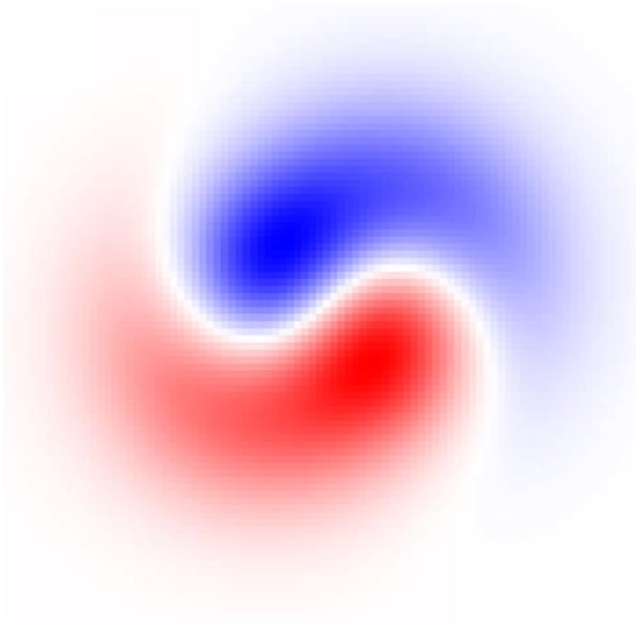

陰
陽

SPICE - Characterization and control of quantum materials with optical vortex beams

Ingelheim, 11/06/2025

Magnetic ~~Helicoidal~~ Dichroism (MHD)
Magnetic Vortex ~~Dichroism~~ (MVD)
Magnetic Vortex Differential Scattering (MVDS)

Mauro Fanciulli

CY Cergy Paris University, DICO LIDYL - CEA Saclay, France

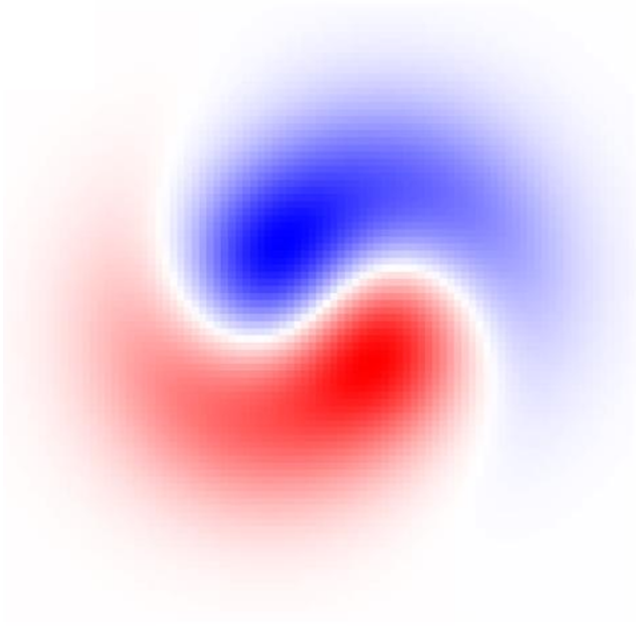

陰
陽

SPICE - Characterization and control of quantum materials with optical vortex beams

Ingelheim, 11/06/2025

Magnetic ~~Helicoidal~~ Dichroism (MHD)
Magnetic Vortex ~~Dichroism~~ (MVD)
~~Magnetic Vortex Differential Scattering (MVDS)~~
Magnetic Vortex Vortex Differential Scattering (MVVDS)

Mauro Fanciulli

CY Cergy Paris University, DICO LIDYL - CEA Saclay, France

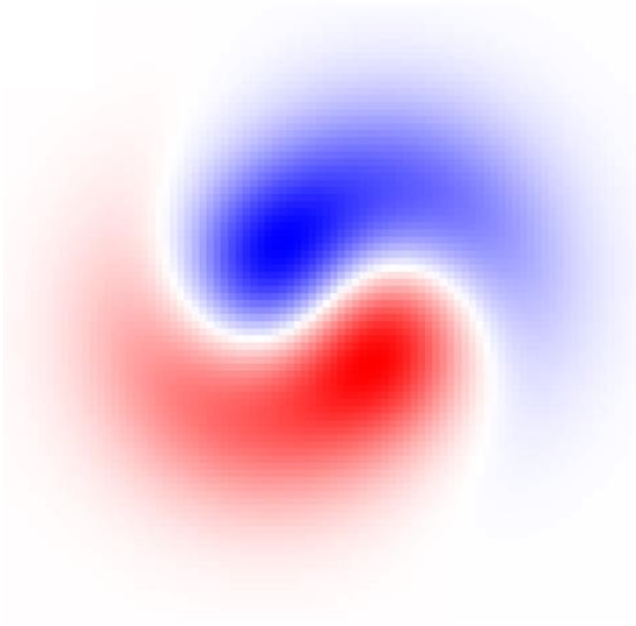

陰
陽

SPICE - Characterization and control of quantum materials with optical vortex beams

Ingelheim, 11/06/2025

Magnetic Helicoidal Dichroism (MHD)

- Introduction

- Analytical description of MHD

  M. Fanciulli et al., PRA 103, 013501 (2021)

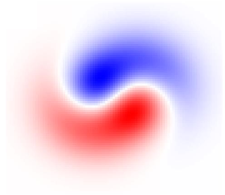

- Static MHD on a magnetic vortex

  M. Fanciulli et al., PRL 128, 077401 (2022)

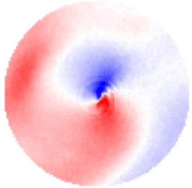

- Pump-probe MHD on a magnetic vortex

  M. Fanciulli et al., PRL 134, 156701 (2025)

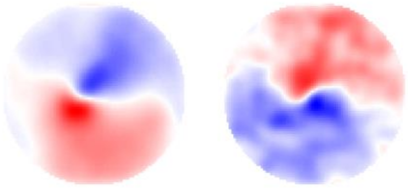

- Conclusions

Magnetic Helicoidal Dichroism (MHD)

- ~~Introduction~~
- Analytical description of MHD

  M. Fanciulli et al., PRA 103, 013501 (2021)

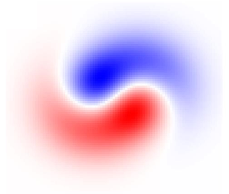

- Static MHD on a magnetic vortex

  M. Fanciulli et al., PRL 128, 077401 (2022)

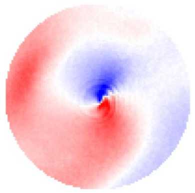

- Pump-probe MHD on a magnetic vortex

  M. Fanciulli et al., PRL 134, 156701 (2025)

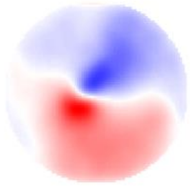

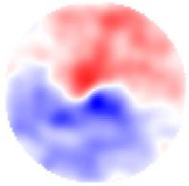

- Conclusions

Q.: what happens in **light-matter interaction** when light carries OAM?

- Fundamental topic
- Measurement technique

Q.: what happens in **light-matter interaction** when light carries OAM?

- Fundamental topic
- Measurement technique

- **Magnetism** can change intensity, polarization and phase of incident light (MOKE, Faraday, Zeeman…)

Q.: what happens in **light-matter interaction** when light carries OAM?

- Fundamental topic
- Measurement technique

➢ **Magnetism** can change intensity, polarization and phase of incident light (MOKE, Faraday, Zeeman…)

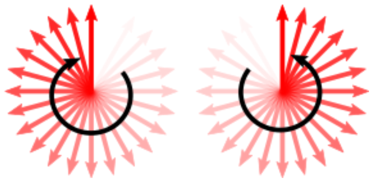

*Switching SAM leads to **dichroic effects** (magnetic circular dichroism, MCD)*

*What happens when switching OAM? (**magnetic helicoidal dichroism**, MHD)*

➢ Case of light scattering from a magnetic target

Analytical description of MHD

- *David Bresteau*
- *Mekha Vimal*
- *Martin Luttmann*
- ***Thierry Ruchon***

- *Maurizio Sacchi*

MOKE formalism

Magneto-Optic Kerr Effect
Change of light polarization and intensity upon reflection by a magnetic target

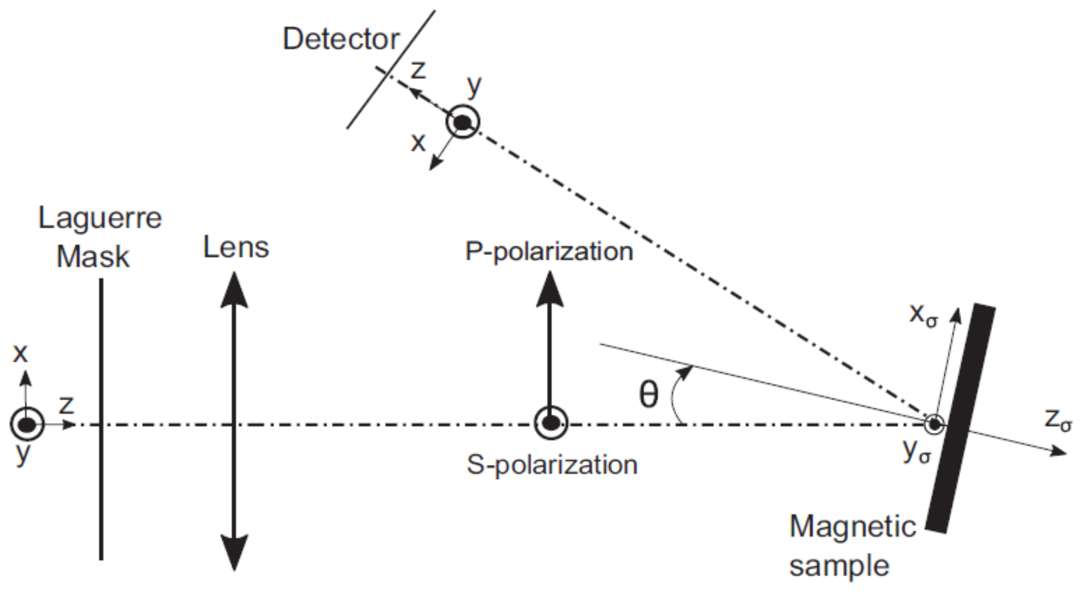

MF et al., PRA 103, 013501 (2021)

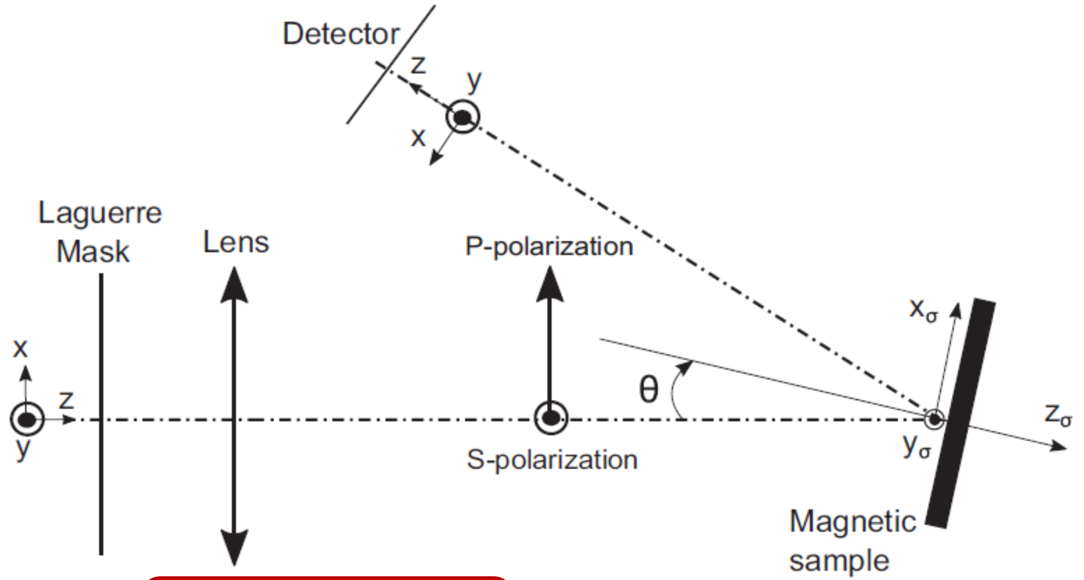

$$\vec{E}_{\text{in}} = A_{\rho}^{|\ell|} e^{i\varphi_0} e^{i\ell\phi} \begin{pmatrix} \epsilon_P \\ \epsilon_S \end{pmatrix}$$

Light with OAM

$$\vec{E}_{\text{in}} = C_{\rho}^{|\ell|} \frac{1}{w(z)} \left(\frac{r\sqrt{2}}{w(z)} \right)^{|\ell|} L_{\rho}^{|\ell|} \left(\frac{2r^2}{w^2(z)} \right) \; e^{-\frac{r^2}{w^2(z)}} e^{-ik\frac{r^2}{2R(z)}} e^{i\ell\phi} e^{i(\omega t - kz)} e^{i(2\rho + |\ell| + 1)\gamma(z)} \begin{pmatrix} \epsilon_P \\ \epsilon_S \end{pmatrix}$$

MF et al., PRA 103, 013501 (2021)

MOKE formalism

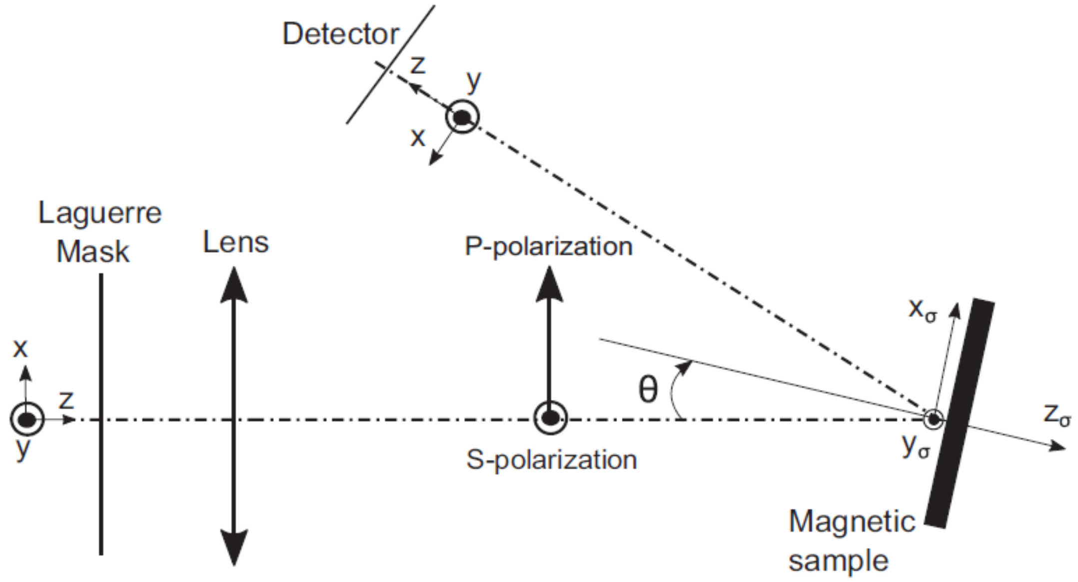

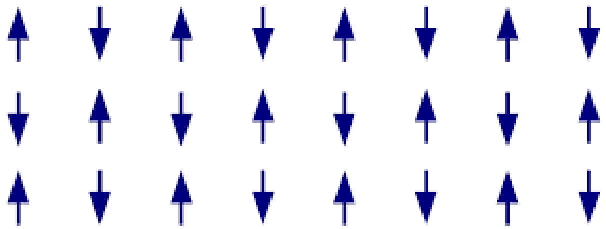

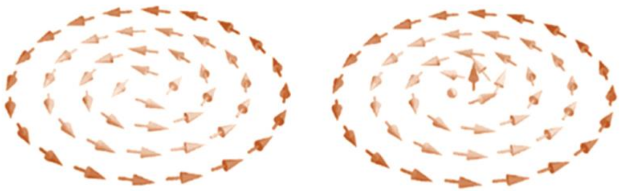

$$\vec{E}_{\text{in}} = A_\rho^{|\ell|} e^{i\varphi_0} e^{i\ell\phi} \begin{pmatrix} \epsilon_P \\ \epsilon_S \end{pmatrix}$$

Magnetic structure symmetry:
Fourier decomposition

$$\vec{m}_l = m_l \hat{x_\sigma}, \ \vec{m}_t = m_t \hat{y_\sigma} \text{ and } \vec{m}_p = m_p \hat{z_\sigma}$$

$$m_*(\phi_\sigma) = \sum_{n=-\infty}^{+\infty} m_{*,n} e^{in\phi_\sigma}$$

$$\text{with } * = l, p, t$$

$$m_{*,n} = \frac{1}{2\pi} \int_0^{2\pi} m_*(\phi_\sigma) e^{-in\phi_\sigma} d\phi_\sigma$$

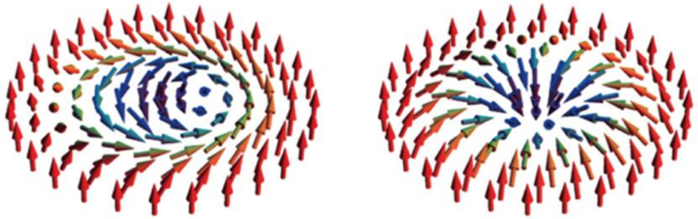

MF et al., PRA 103, 013501 (2021)

MOKE formalism

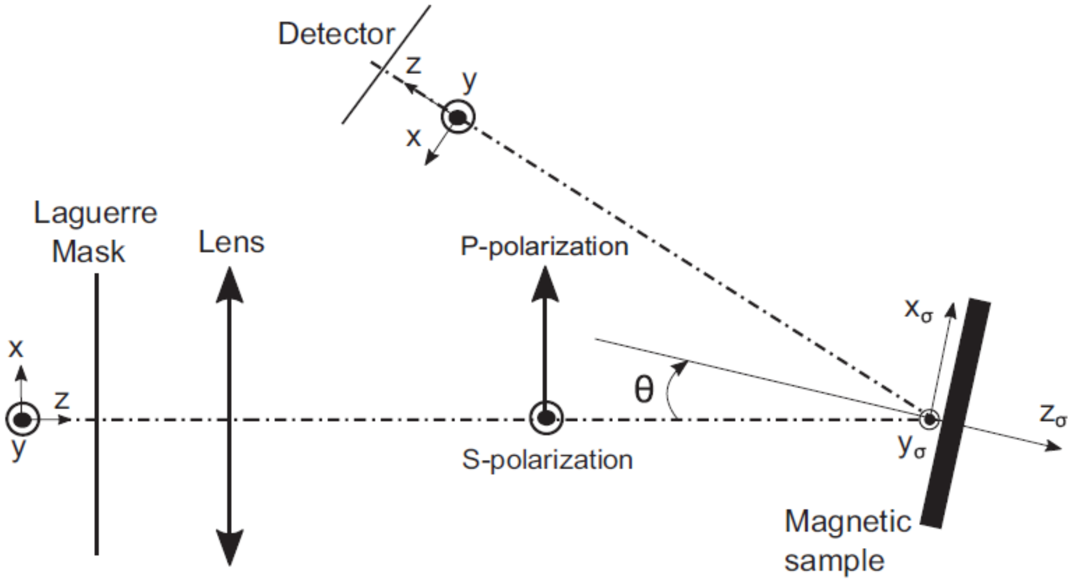

$$\vec{E}_{\text{in}} = A_\rho^{|\ell|} e^{i\varphi_0} e^{i\ell\phi} \begin{pmatrix} \epsilon_P \\ \epsilon_S \end{pmatrix}$$

$$\vec{m}_l = m_l \hat{x_\sigma}, \ \vec{m}_t = m_t \hat{y_\sigma} \text{ and } \vec{m}_p = m_p \hat{z_\sigma}$$

$$m_*(\phi_\sigma) = \sum_{n=-\infty}^{+\infty} m_{*,n} e^{in\phi_\sigma}$$

with $* = l, p, t$

$$m_{*,n} = \frac{1}{2\pi} \int_0^{2\pi} m_*(\phi_\sigma) e^{-in\phi_\sigma} d\phi_\sigma$$

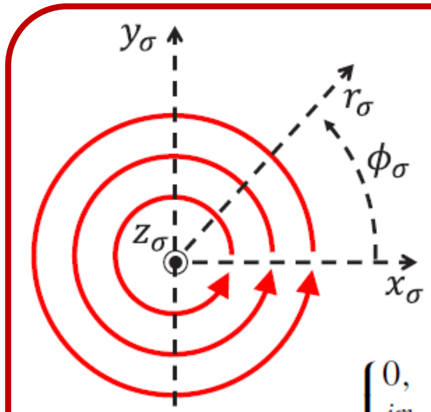

$$m_l(\phi_\sigma) = -m_0 \sin \phi_\sigma$$

$$m_t(\phi_\sigma) = m_0 \cos \phi_\sigma$$

$$m_{*,n} = \begin{cases} 0, & \text{for } n \neq \pm 1 \\ \frac{im_0}{2} n, & \text{for } n = \pm 1, * = l \\ \frac{m_0}{2}, & \text{for } n = \pm 1, * = t \end{cases}$$

MF et al., PRA 103, 013501 (2021)

MOKE formalism

$$\mathbf{R} = \begin{pmatrix} r_{PP}\cdot\left[1 + r_0^t\cdot m_t\right] & r_{PS}^l\cdot m_l + r_{PS}^p\cdot m_p \\ -r_{PS}^l\cdot m_l + r_{PS}^p\cdot m_p & r_{SS} \end{pmatrix}$$

$$\vec{E}_{\text{out}} = \mathbf{R}\vec{E}_{\text{in}}$$

MOKE

$$\vec{E}_{\text{out}} = \sum_n \vec{E}_{n,\ell} = A_\rho^{|\ell|}(r,0)e^{i\varphi_0}\sum_n e^{i(\ell\phi + n\phi_\sigma)}\begin{pmatrix}\alpha_{n,m}^x \\ \alpha_{n,m}^y\end{pmatrix}$$

Near field reflection

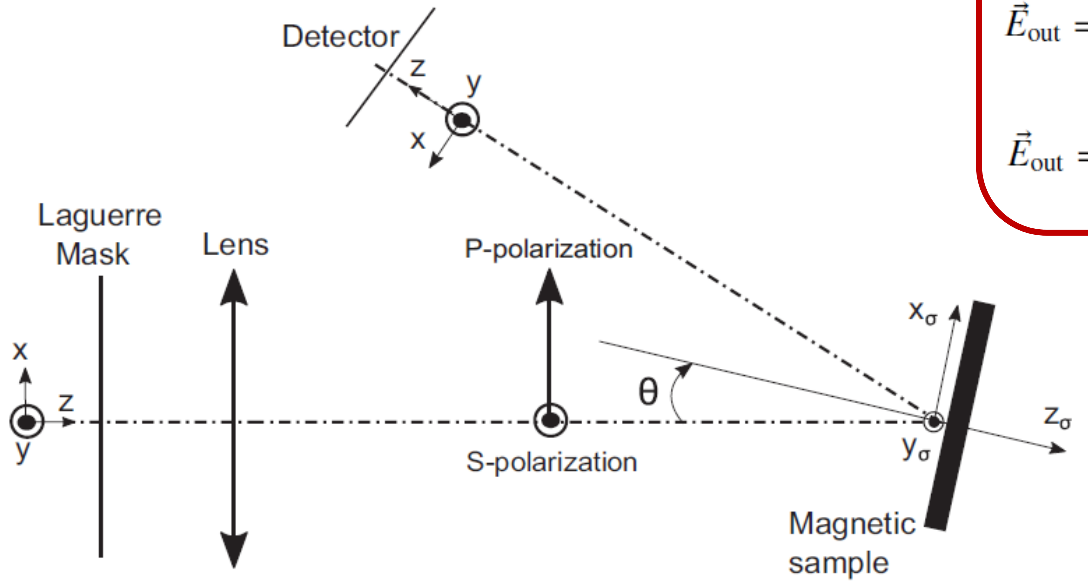

$$\vec{E}_{\text{in}} = A_\rho^{|\ell|}e^{i\varphi_0}e^{i\ell\phi}\begin{pmatrix}\epsilon_P \\ \epsilon_S\end{pmatrix}$$

$$\vec{m}_l = m_l\hat{x_\sigma},\ \vec{m}_t = m_t\hat{y_\sigma} \text{ and } \vec{m}_p = m_p\hat{z_\sigma}$$

$$m_*(\phi_\sigma) = \sum_{n=-\infty}^{+\infty} m_{*,n}e^{in\phi_\sigma}$$

$$\text{with } * = l, p, t$$

$$m_{*,n} = \frac{1}{2\pi}\int_0^{2\pi} m_*(\phi_\sigma)e^{-in\phi_\sigma}\,d\phi_\sigma$$

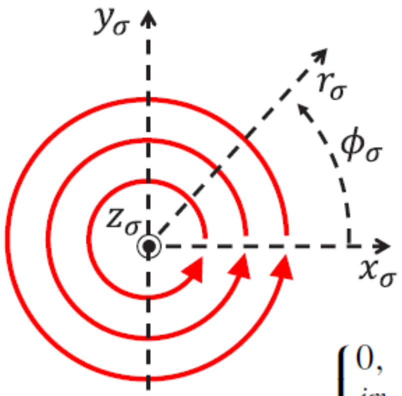

$$m_l(\phi_\sigma) = -m_0\sin\phi_\sigma$$

$$m_t(\phi_\sigma) = m_0\cos\phi_\sigma$$

$$m_{*,n} = \begin{cases} 0, & \text{for } n \neq \pm 1 \\ \frac{im_0}{2}n, & \text{for } n = \pm 1, * = l \\ \frac{m_0}{2}, & \text{for } n = \pm 1, * = t \end{cases}$$

MF et al., PRA 103, 013501 (2021)

MOKE formalism

$$E(t,r,\phi,z)=\frac{e^{i\varphi_0(t,z)}}{i\lambda z}\,e^{\frac{ik}{2z}r^2}\int_0^{2\pi}d\phi'\int_0^{+\infty}r'dr'\,E(r',\phi',0)e^{-\frac{ikrr'}{z}\cos(\phi-\phi')}$$

$$I^{x,y}_{\ell,m}=\left|\sum_n E^{x,y}_{n,\ell,m}\right|^2$$

Fresnel propagation

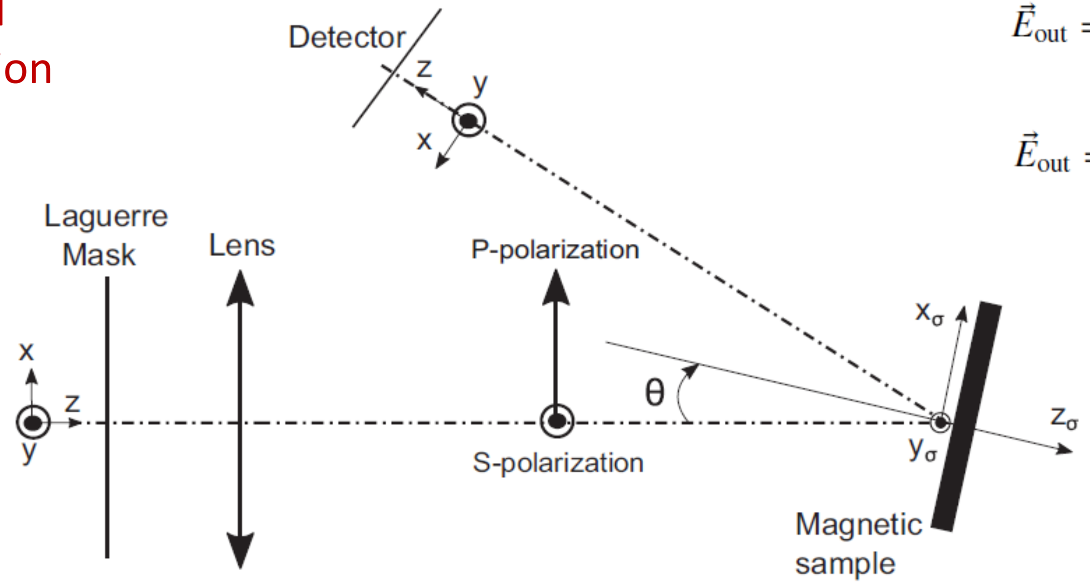

$$\mathbf{R}=\begin{pmatrix} r_{PP}\cdot[1+r_0^t\cdot m_t] & r^l_{PS}\cdot m_l+r^p_{PS}\cdot m_p \\ -r^l_{PS}\cdot m_l+r^p_{PS}\cdot m_p & r_{SS}\end{pmatrix}$$

$$\vec{E}_{\text{out}}=\mathbf{R}\vec{E}_{\text{in}}$$

$$\vec{E}_{\text{out}}=\sum_n \vec{E}_{n,\ell}=A^{|\ell|}_\rho(r,0)e^{i\varphi_0}\sum_n e^{i(\ell\phi+n\phi_\sigma)}\begin{pmatrix}\alpha^x_{n,m}\\ \alpha^y_{n,m}\end{pmatrix}$$

$$\vec{E}_{\text{in}}=A^{|\ell|}_\rho e^{i\varphi_0}e^{i\ell\phi}\begin{pmatrix}\epsilon_P\\ \epsilon_S\end{pmatrix}$$

$$\vec{m}_l=m_l\hat{x_\sigma},\ \vec{m}_t=m_t\hat{y_\sigma}\ \text{and}\ \vec{m}_p=m_p\hat{z_\sigma}$$

$$m_*(\phi_\sigma)=\sum_{n=-\infty}^{+\infty}m_{*,n}e^{in\phi_\sigma}$$

with $*=l,p,t$

$$m_{*,n}=\frac{1}{2\pi}\int_0^{2\pi}m_*(\phi_\sigma)e^{-in\phi_\sigma}d\phi_\sigma$$

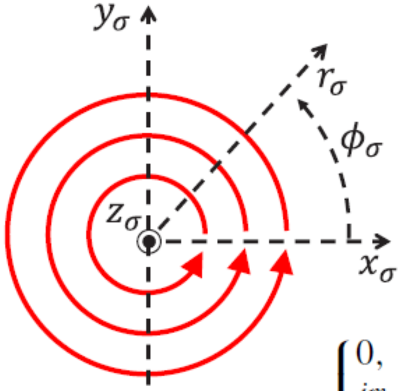

$$m_l(\phi_\sigma)=-m_0\sin\phi_\sigma$$

$$m_t(\phi_\sigma)=m_0\cos\phi_\sigma$$

$$m_{*,n}=\begin{cases}0, & \text{for } n\neq\pm1\\ \frac{im_0}{2}n, & \text{for } n=\pm1, *=l\\ \frac{m_0}{2}, & \text{for } n=\pm1, *=t\end{cases}$$

MF et al., PRA 103, 013501 (2021)

MOKE formalism

$$E(t,r,\phi,z) = \frac{e^{i\varphi_0(t,z)}}{i\lambda z}\, e^{\frac{ik}{2z}r^2}\int_0^{2\pi} d\phi' \int_0^{+\infty} r'dr'\, E(r',\phi',0)e^{-\frac{ikrr'}{z}\cos(\phi-\phi')}$$

$$I^{x,y}_{\ell,m} = \left|\sum_n E^{x,y}_{n,\ell,m}\right|^2$$

$$\mathbf{R} = \begin{pmatrix} r_{PP}\cdot[1+r_0^t\cdot m_t] & r_{PS}^l\cdot m_l + r_{PS}^p\cdot m_p \\ -r_{PS}^l\cdot m_l + r_{PS}^p\cdot m_p & r_{SS}\end{pmatrix}$$

$$\vec{E}_{\text{out}} = \mathbf{R}\vec{E}_{\text{in}}$$

$$\vec{E}_{\text{out}} = \sum_n \vec{E}_{n,\ell} = A_\rho^{|\ell|}(r,0)e^{i\varphi_0}\sum_n e^{i(\ell\phi+n\phi_\sigma)}\begin{pmatrix}\alpha^x_{n,m}\\ \alpha^y_{n,m}\end{pmatrix}$$

$\ell + n$

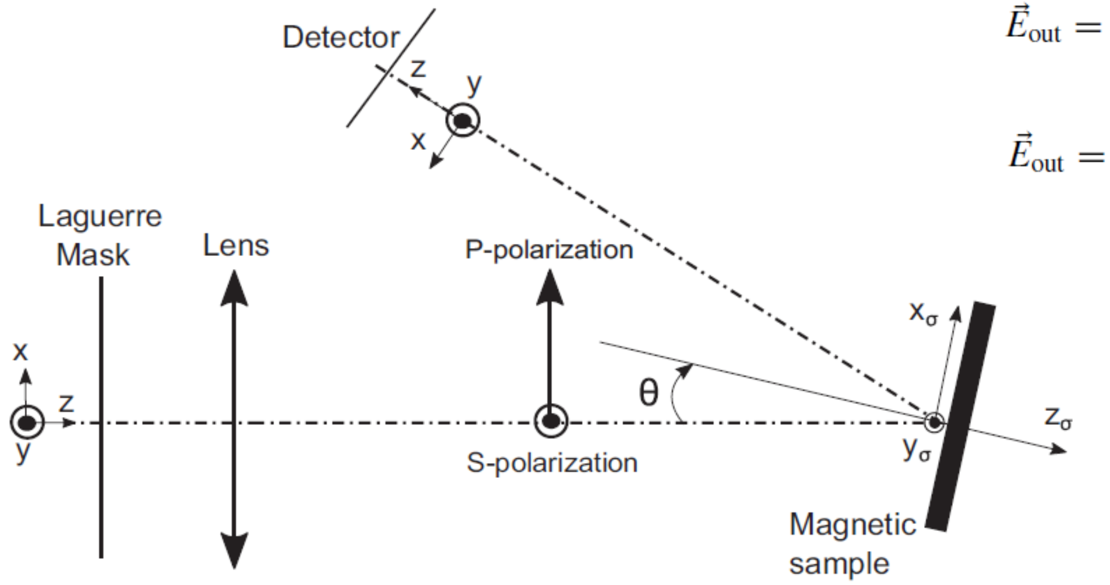

$\ell_{in} = 1$

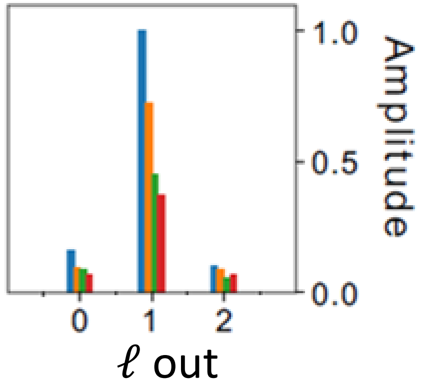

$$\vec{E}_{\text{in}} = A_\rho^{|\ell|}e^{i\varphi_0}e^{i\ell\phi}\begin{pmatrix}\epsilon_P\\ \epsilon_S\end{pmatrix}$$

ℓ

Also for ℓ =0 !

$$\vec{m}_l = m_l\hat{x_\sigma},\ \vec{m}_t = m_t\hat{y_\sigma} \text{ and } \vec{m}_p = m_p\hat{z_\sigma}$$

$$m_*(\phi_\sigma) = \sum_{n=-\infty}^{+\infty} m_{*,n}e^{in\phi_\sigma}$$

with $* = l, p, t$

$$m_{*,n} = \frac{1}{2\pi}\int_0^{2\pi} m_*(\phi_\sigma)e^{-in\phi_\sigma}d\phi_\sigma$$

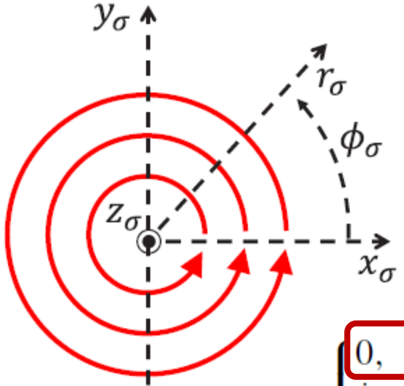

$$m_l(\phi_\sigma) = -m_0\sin\phi_\sigma$$

$$m_t(\phi_\sigma) = m_0\cos\phi_\sigma$$

$$m_{*,n} = \begin{cases} 0, & \text{for } n \neq \pm 1 \\ \frac{im_0}{2}n, & \text{for } n = \pm 1, * = l \\ \frac{m_0}{2}, & \text{for } n = \pm 1, * = t \end{cases}$$

MF et al., PRA 103, 013501 (2021)

Three types of magnetic helicoidal dichroism (MHD)

$$\mathrm{MHD}\ell = \left(I_{\ell,m} - I_{-\ell,m}\right) / \left(I_{\ell,m} + I_{-\ell,m}\right)$$
$$\mathrm{MHD}m = \left(I_{\ell,m} - I_{\ell,-m}\right) / \left(I_{\ell,m} + I_{\ell,-m}\right)$$

MF et al., PRA 103, 013501 (2021)

Three types of magnetic helicoidal dichroism (MHD)

$$\mathrm{MHD}\ell = (I_{\ell,m} - I_{-\ell,m}) \,/\, (I_{\ell,m} + I_{-\ell,m})$$
$$\mathrm{MHD}m = (I_{\ell,m} - I_{\ell,-m}) \,/\, (I_{\ell,m} + I_{\ell,-m})$$
$$\mathrm{MHD}\ell m = (I_{\ell,m} - I_{-\ell,-m}) \,/\, (I_{\ell,m} + I_{-\ell,-m})$$

$$\boxed{\mathrm{MHD}\ell = \mathrm{MHD}\ell m + \mathrm{MHD}m}$$

MF et al., PRA 103, 013501 (2021)

Three types of magnetic helicoidal dichroism (MHD)

$$\mathrm{MHD}\ell = (I_{\ell,m} - I_{-\ell,m}) \,/\, (I_{\ell,m} + I_{-\ell,m})$$
$$\mathrm{MHD}m = (I_{\ell,m} - I_{\ell,-m}) \,/\, (I_{\ell,m} + I_{\ell,-m})$$
$$\mathrm{MHD}\ell m = (I_{\ell,m} - I_{-\ell,-m}) \,/\, (I_{\ell,m} + I_{-\ell,-m})$$

$$\Delta I_{\ell}^{x,y}(r,\phi,z) = 2\left|D_{\rho}^{|\ell|}\right|^2 \sum_{\substack{n \neq n' \\ n-n'>0}} H_{n,\ell}(kr,z) H_{n',\ell}(kr,z) \times \left[\left|\alpha_{n,m}^{x,y}\right|\left|\alpha_{n',m}^{x,y}\right| \cos\left((n-n')(\phi-\pi/2)+\delta\varphi_{n,n'}^{x,y}\right) - (-1)^{n+n'}\left|\alpha_{-n,m}^{x,y}\right|\left|\alpha_{-n',m}^{x,y}\right| \cos\left((n-n')(\phi-\pi/2) - \delta\varphi_{-n,-n'}^{x,y}\right)\right],$$

$$\Delta I_{m}^{x,y}(r,\phi,z) = 4\left|D_{\rho}^{|\ell|}\right|^2 \sum_{n\neq 0} \left|\alpha_{0,m}^{x,y}\right|\left|\alpha_{n,m}^{x,y}\right| \times \cos\left[n(\phi-\pi/2)+\delta\varphi_{n,0}^{x,y}\right] H_{0,\ell}(kr,z) H_{n,\ell}(kr,z),$$

$$\Delta I_{\ell,m}^{x,y}(r,\phi,z) = 2\left|D_{\rho}^{|\ell|}\right|^2 \sum_{\substack{n \neq n' \\ n-n'>0}} H_{n,\ell}(kr,z) H_{n',\ell}(kr,z) \times \left[\left|\alpha_{n,m}^{x,y}\right|\left|\alpha_{n',m}^{x,y}\right| \cos\left((n-n')(\phi-\pi/2)+\delta\varphi_{n,n'}^{x,y}\right) + \chi_{n,n'}(-1)^{n+n'}\left|\alpha_{-n,m}^{x,y}\right|\left|\alpha_{-n',m}^{x,y}\right| \times \cos\left((n-n')(\phi-\pi/2) - \delta\varphi_{-n,-n'}^{x,y}\right)\right].$$

$$\mathrm{MHD}\ell = \mathrm{MHD}\ell m + \mathrm{MHD}m$$

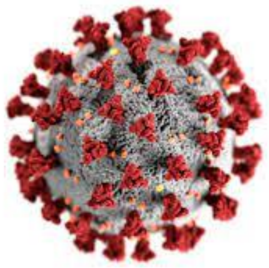

MF et al., PRA 103, 013501 (2021)

Three types of magnetic helicoidal dichroism (MHD)

***Magnetic Vortex* Vortex Differential Scattering (MVVDS)**

$$\mathrm{MHD}\ell = (I_{\ell,m} - I_{-\ell,m}) \,/\, (I_{\ell,m} + I_{-\ell,m})$$

$$\mathrm{MHD}m = (I_{\ell,m} - I_{\ell,-m}) \,/\, (I_{\ell,m} + I_{\ell,-m})$$

$$\mathrm{MHD}\ell m = (I_{\ell,m} - I_{-\ell,-m}) \,/\, (I_{\ell,m} + I_{-\ell,-m})$$

$$\mathrm{MHD}\ell = \mathrm{MHD}\ell m + \mathrm{MHD}m$$

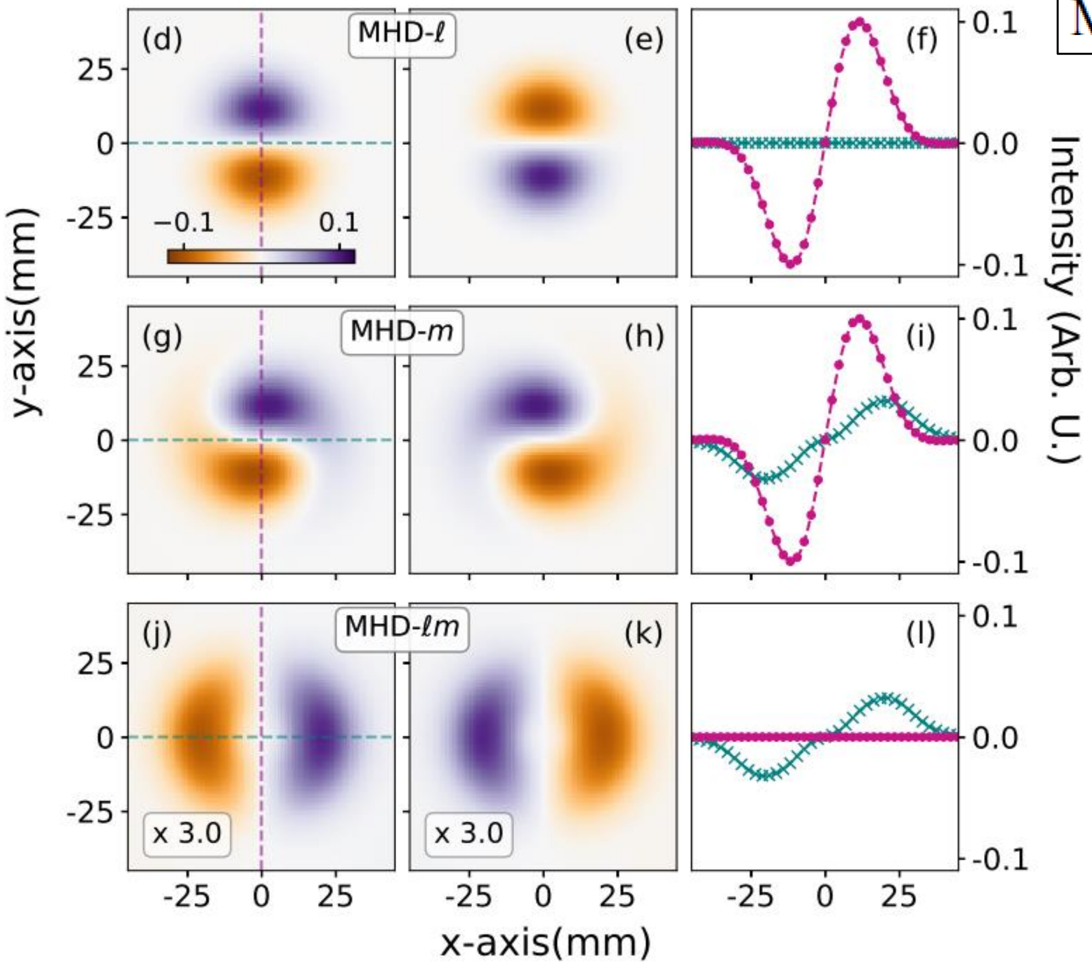

MF et al., PRA 103, 013501 (2021)

Actually…

Actually…

- $A + R + T = 1 \rightarrow$ *for a bulky sample:* $A = 1 - R$

Actually…

- $A + R + T = 1 \rightarrow$ *for a bulky sample:* $A = 1 - R$
- *Helical* $\neq$ *Helicoidal !!!*

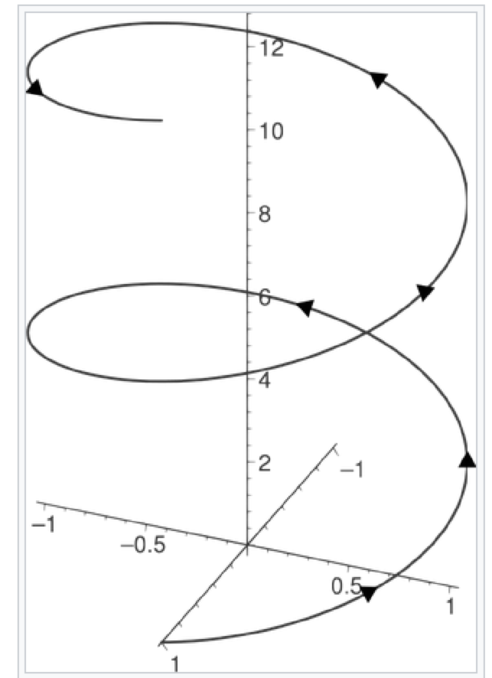

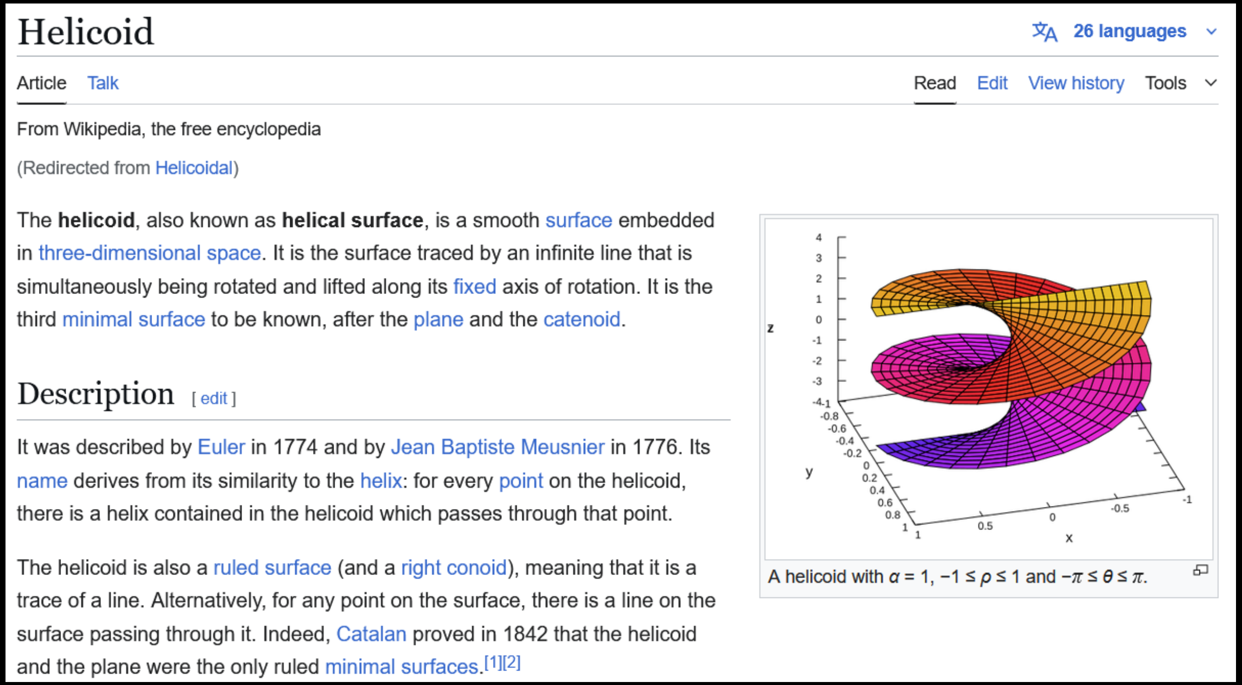

Helicoid

26 languages

Article Talk

Read Edit View history Tools

From Wikipedia, the free encyclopedia

(Redirected from Helicoidal)

The **helicoid**, also known as **helical surface**, is a smooth surface embedded in three-dimensional space. It is the surface traced by an infinite line that is simultaneously being rotated and lifted along its fixed axis of rotation. It is the third minimal surface to be known, after the plane and the catenoid.

Description [edit]

It was described by Euler in 1774 and by Jean Baptiste Meusnier in 1776. Its name derives from its similarity to the helix: for every point on the helicoid, there is a helix contained in the helicoid which passes through that point.

The helicoid is also a ruled surface (and a right conoid), meaning that it is a trace of a line. Alternatively, for any point on the surface, there is a line on the surface passing through it. Indeed, Catalan proved in 1842 that the helicoid and the plane were the only ruled minimal surfaces.[1][2]

A helicoid with $\alpha = 1$, $-1 \leq \rho \leq 1$ and $-\pi \leq \theta \leq \pi$.

Static MHD on a magnetic vortex

CEA PARIS-SACLAY

- Martin Luttmann
- David Bresteau
- Mekha Vimal
- ***Thierry Ruchon***

- Ricardo Sousa
- Laurent Vila
- Ioan-Lucian Prejbeanu
- ***Bernard Dieny***

Elettra Sincrotrone Trieste

- ***Matteo Pancaldi***
- Emanuele Pedersoli
- Dario De Angelis
- Primoz Rebernik Ribic
- Carlo Spezzani
- Michele Manfredda
- ***Giovanni De Ninno***
- ***Flavio Capotondi***

SORBONNE UNIVERSITÉ

- ***Maurizio Sacchi***

PAUL SCHERRER INSTITUT PSI

- Benedikt Rösner
- ***Christian David***

Experimental setup

DiProI beamline
FERMI FEL light source
Trieste, Italy

Al_2O_3-capped permalloy ($Fe_{20}Ni_{80}$), 15um diameter, 80nm thick

50 Hz
52.8 eV (*Fe 3p→3d*)
π pol.
50 fs
4µm FWHM

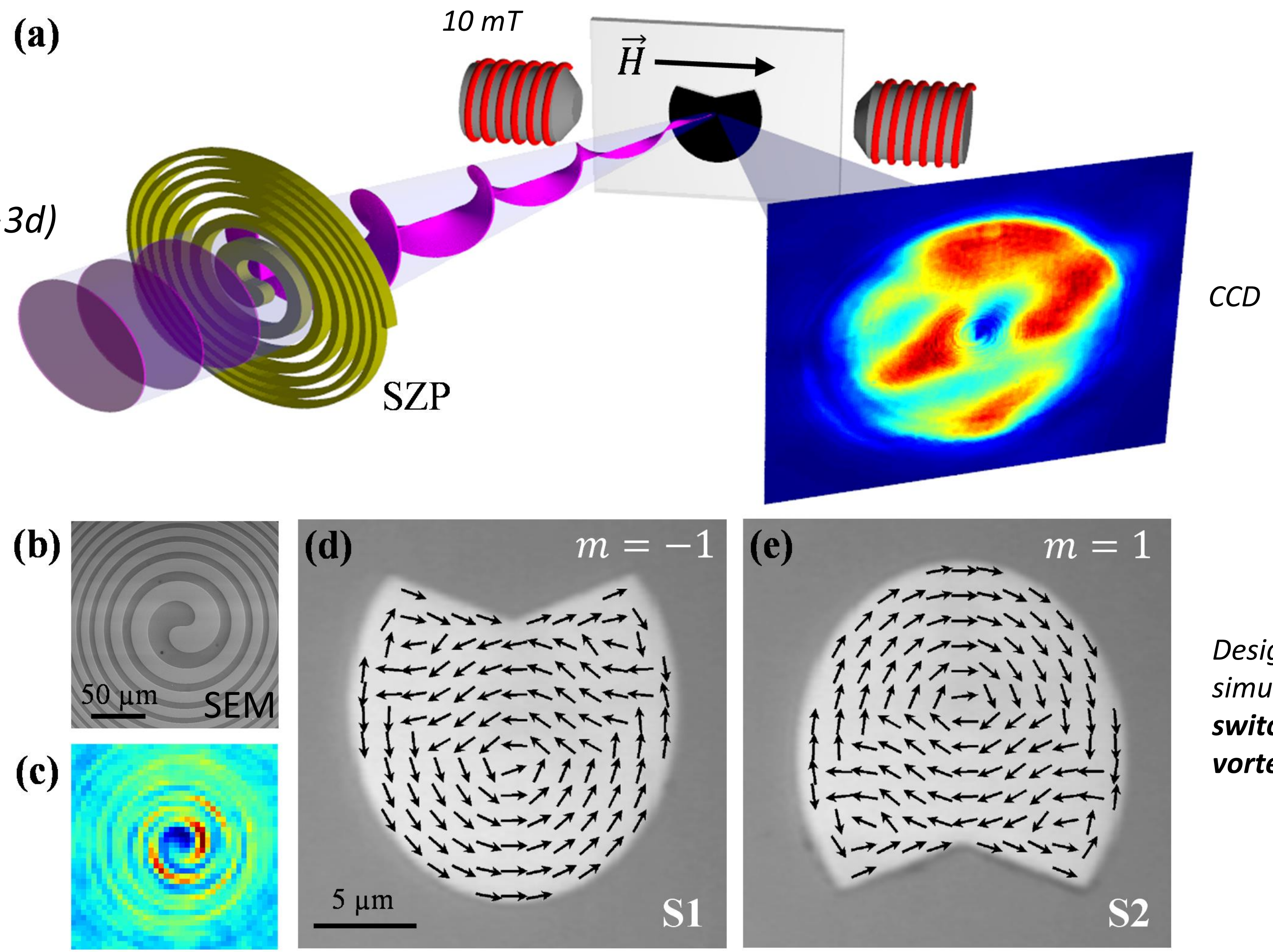

Designed by micromagnetic simulations (OOMMF) for a ***switchable magnetic vortex configuration***

MF et al., PRL 128, 077401 (2022)

MHDm

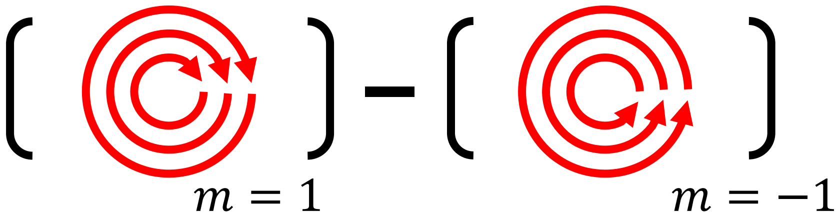

MF et al., PRL 128, 077401 (2022)

MHD"m"

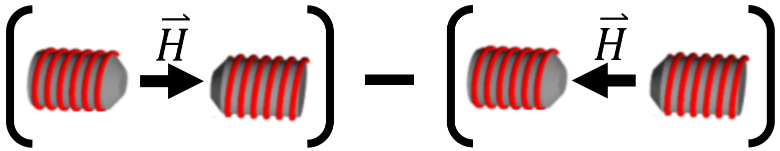

S1

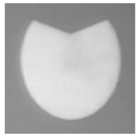

S2

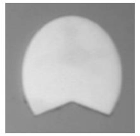

MF et al., PRL 128, 077401 (2022)

MHD"m"

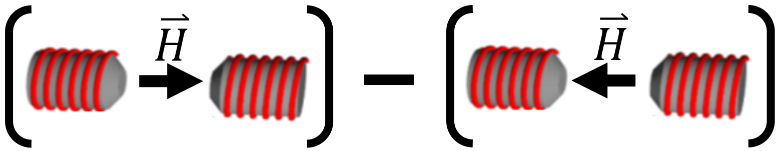

Theory

S1

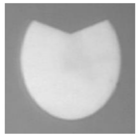

S2

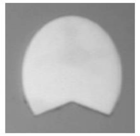

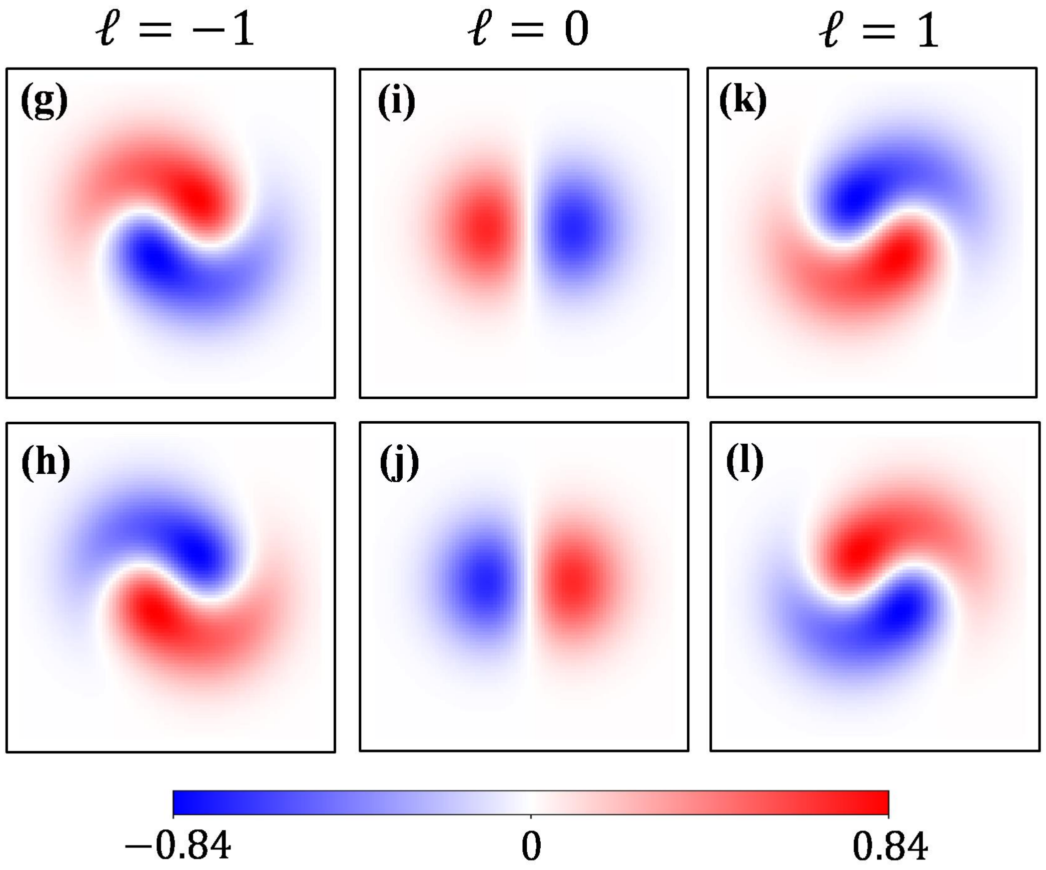

MF et al., PRL 128, 077401 (2022)

MHD"m"

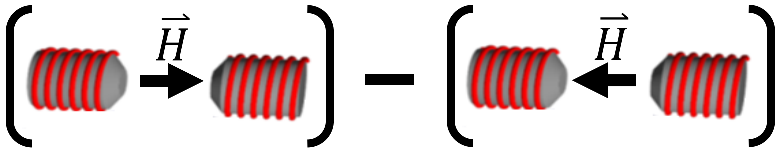

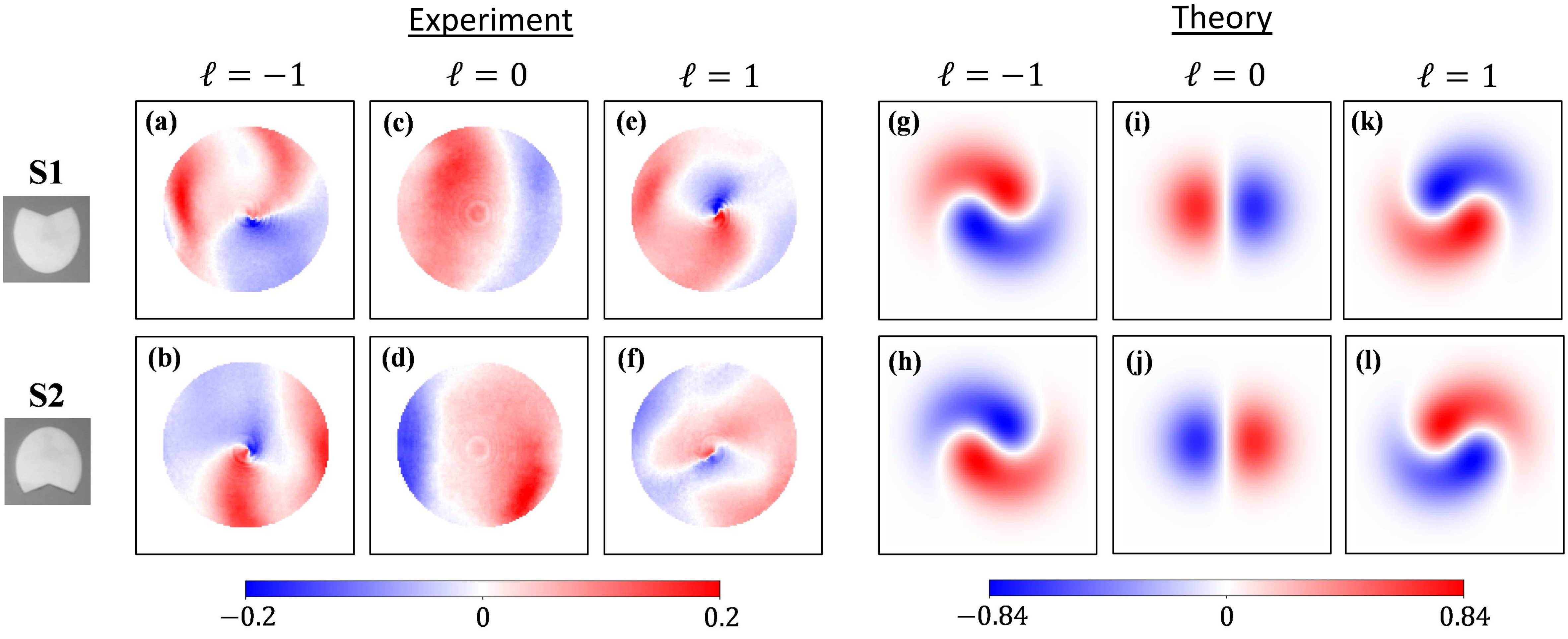

MF et al., PRL 128, 077401 (2022)

MHD"m"

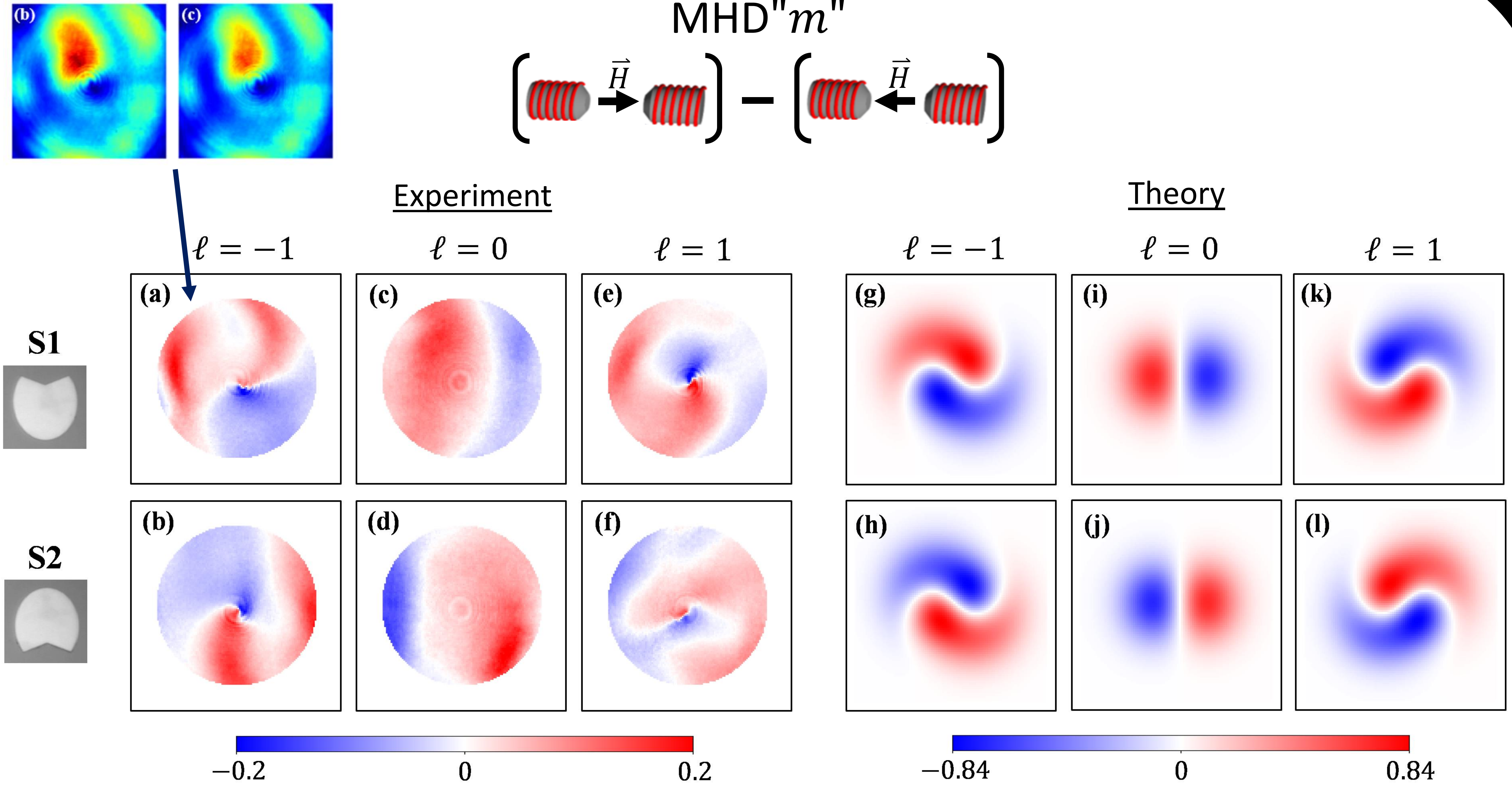

MF et al., PRL 128, 077401 (2022)

Understanding MHD

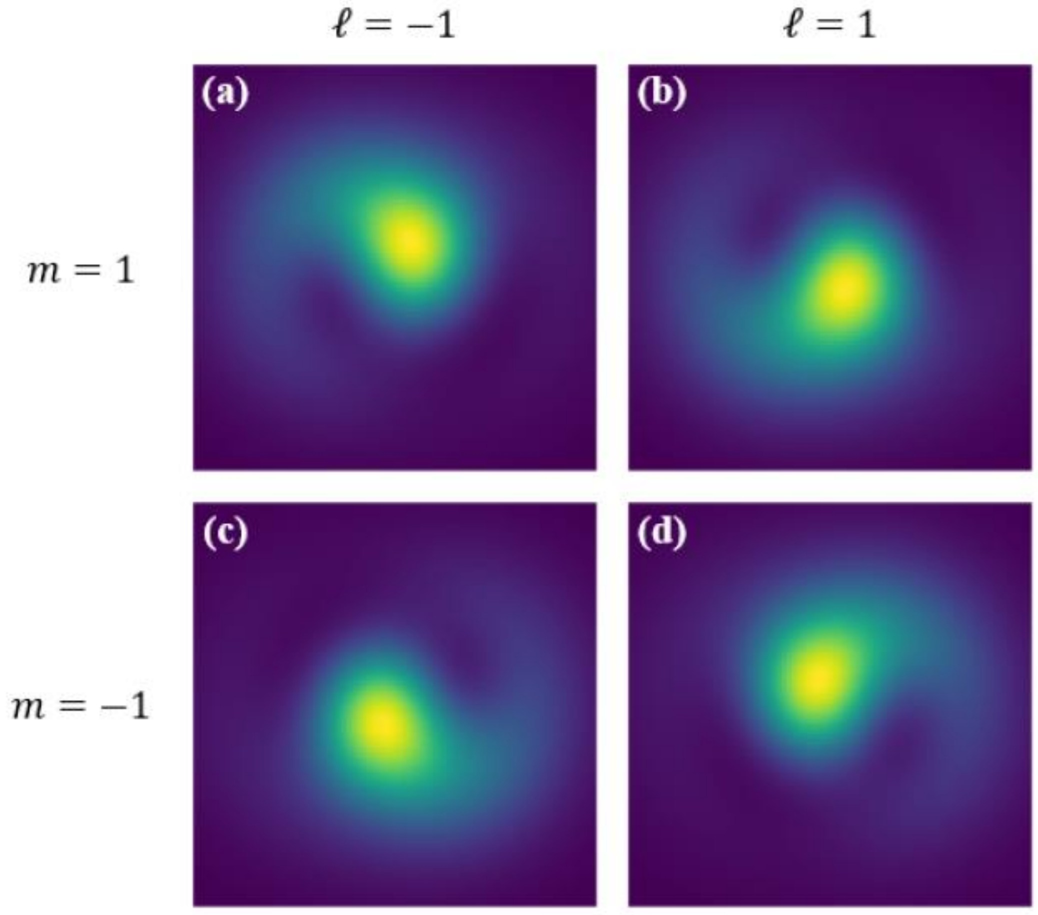

Magnetic vortex
π pol.
52.8 eV
48°

MF et al., PRA 103, 013501 (2021)

Understanding MHD

Simulated far-field reflected intensity

Numerical suppression of the outgoing mode $\ell_{out} = \ell_{in}$

$\forall \ell_{in}$: *also for* $\ell_{in} = 0$ *(!!!)*

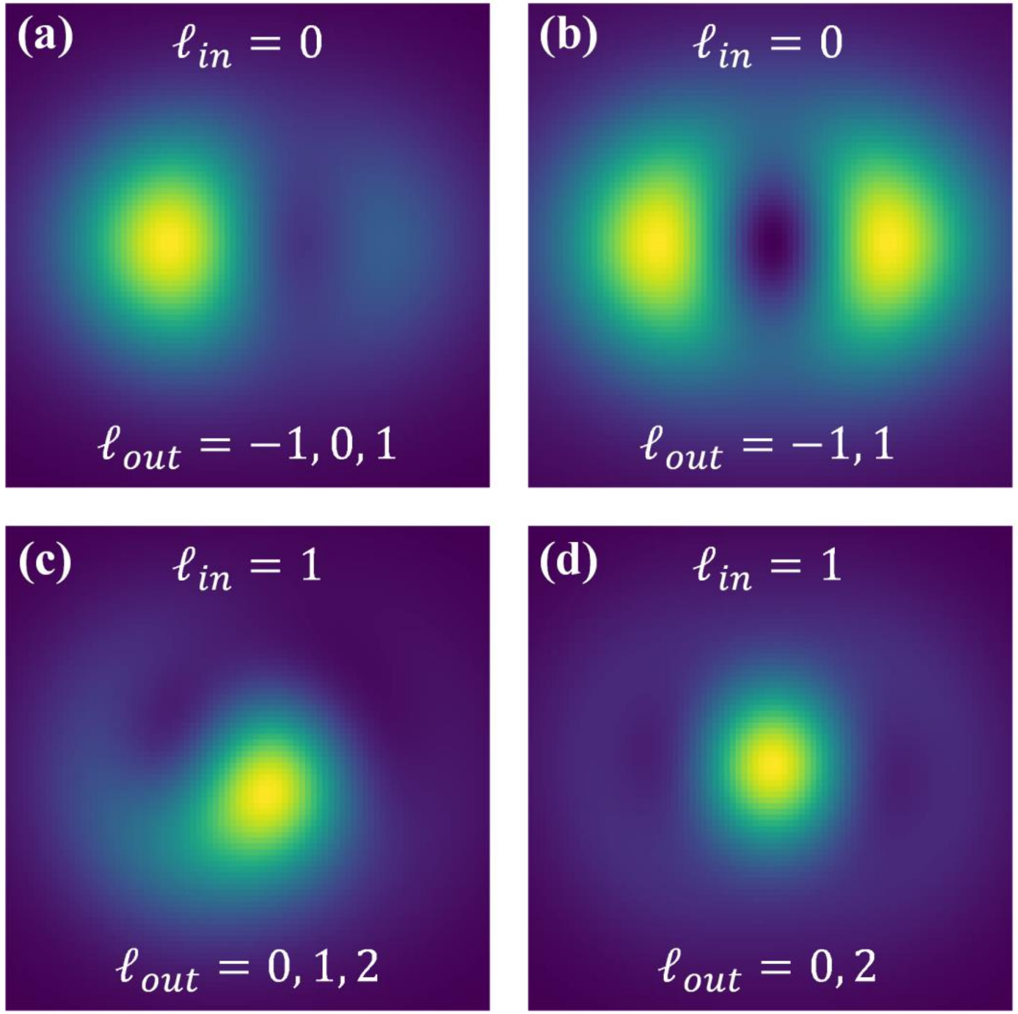

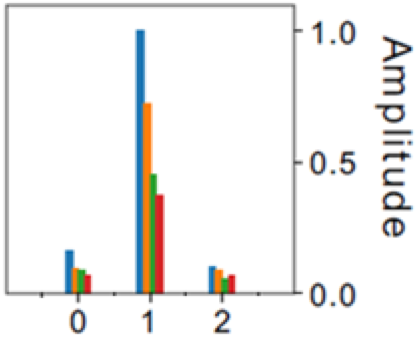

MF et al., PRA 103, 013501 (2021)

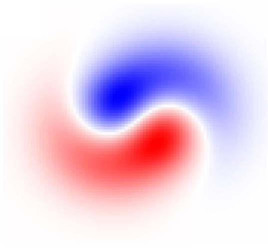

MHD:

- Not easy, but feasible and reproducible
- Sensitive to overall magnetic topology within the probe beam

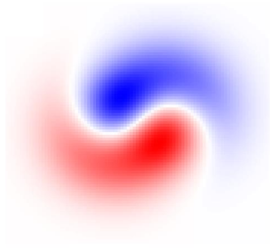

MHD:

- Not easy, but feasible and reproducible
- Sensitive to overall magnetic topology within the probe beam

Next:

- Exploit the time structure of light sources to extend to the ultrafast time domain in **pump-probe** experiments to study **femtosecond magnetic dynamics**
- Exploration of **other physical processes** and **techniques**

Pump-probe MHD on a magnetic vortex

CEA PARIS-SACLAY

- Mathieu Guer
- Martin Luttmann
- David Bresteau
- ***Thierry Ruchon***

- *Anda-Elena Stanciu*
- *Ricardo Sousa*
- *Laurent Vila*
- *Ioan-Lucian Prejbeanu*
- *Liliana D. Buda-Prejbeanu*
- ***Bernard Dieny***

Elettra Sincrotrone Trieste

- ***Matteo Pancaldi***
- *Emanuele Pedersoli*
- *Dario De Angelis*
- *Primoz Rebernik Ribic*
- *Arun Ravindran*
- *Carlo Spezzani*
- *Michele Manfredda*
- ***Giovanni De Ninno***
- ***Flavio Capotondi***

SORBONNE UNIVERSITÉ

- *Pietro Carrara*
- ***Maurizio Sacchi***

PAUL SCHERRER INSTITUT PSI

- *Benedikt Rösner*
- ***Christian David***

tMHD

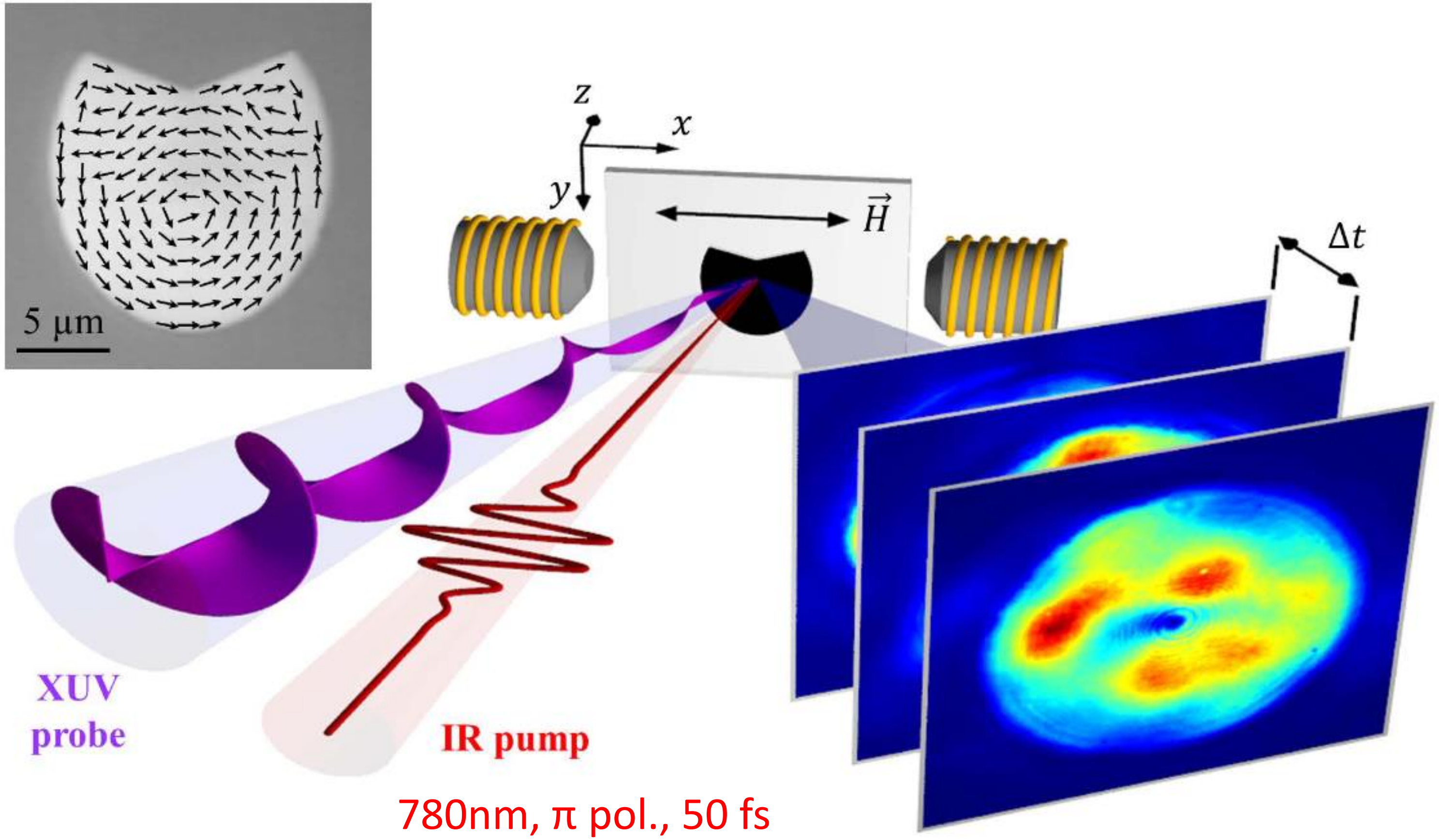

780nm, π pol., 50 fs

MF et al., PRL 134, 156701 (2025)

static

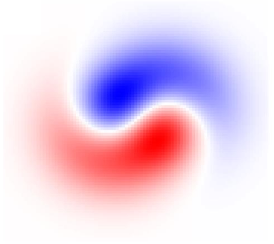

MHD"m"

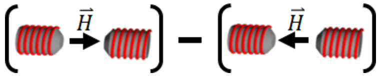

time-resolved

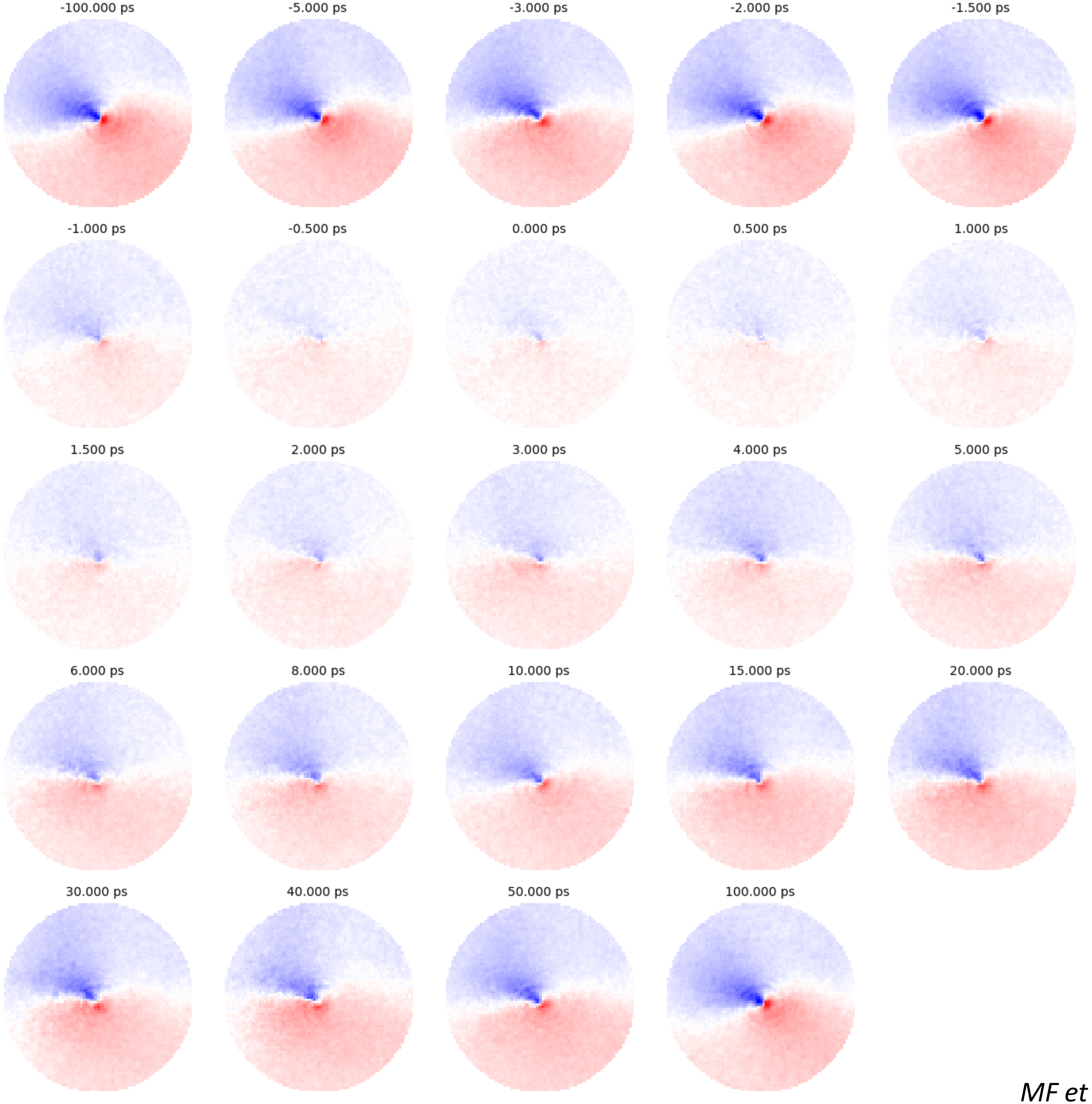

E. Beaurepaire et al., PRL 76, 22 (1996)

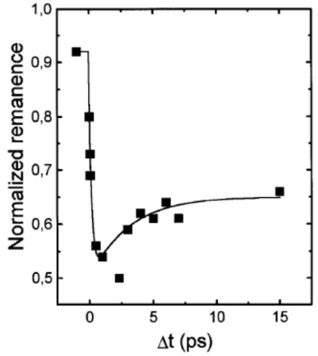

Typical ultrafast demagnetization and remagnetization of Py

MF et al., PRL 134, 156701 (2025)

time-resolved

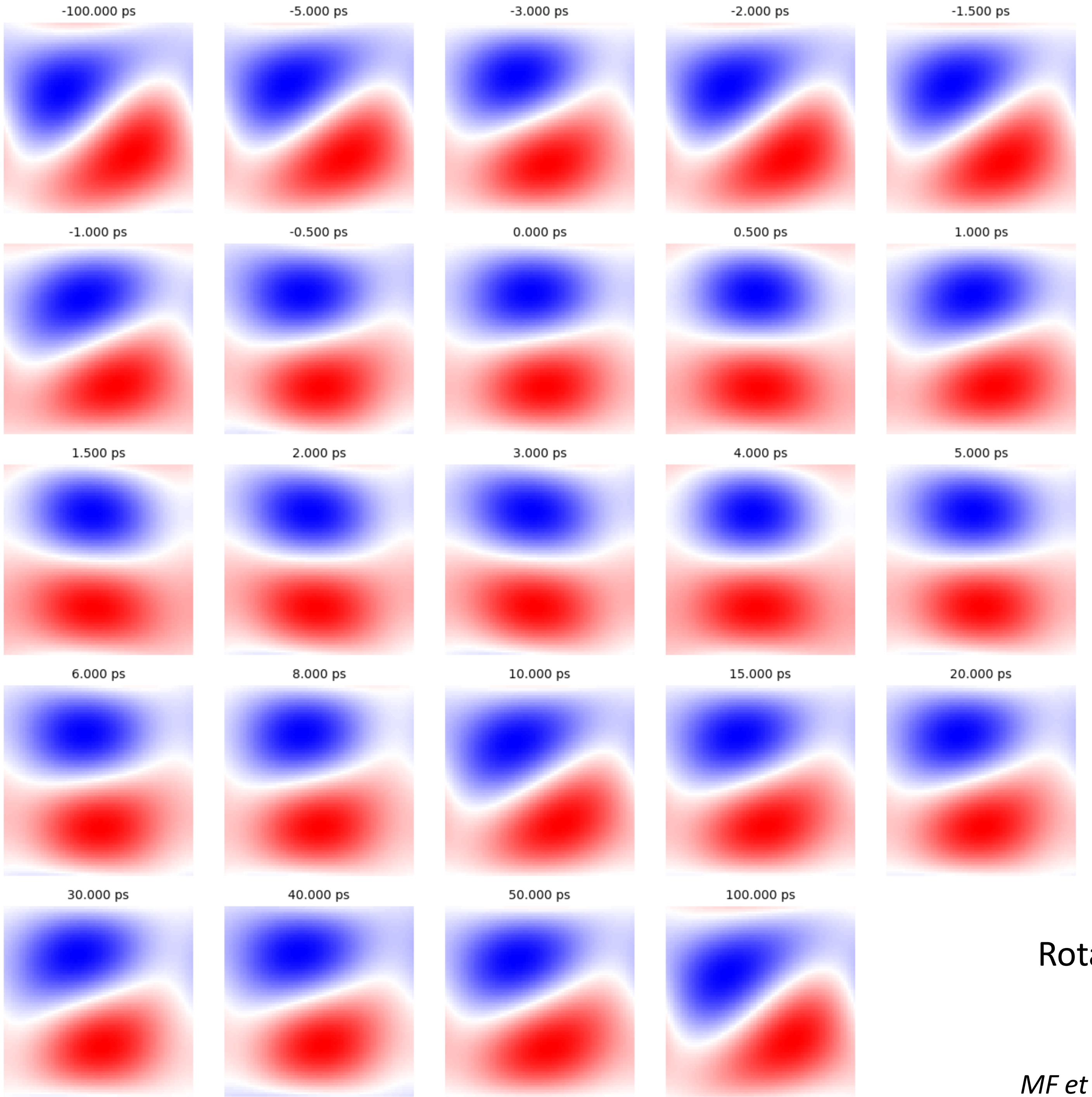

Rotation of MHD signal!

MF et al., PRL 134, 156701 (2025)

tMHD

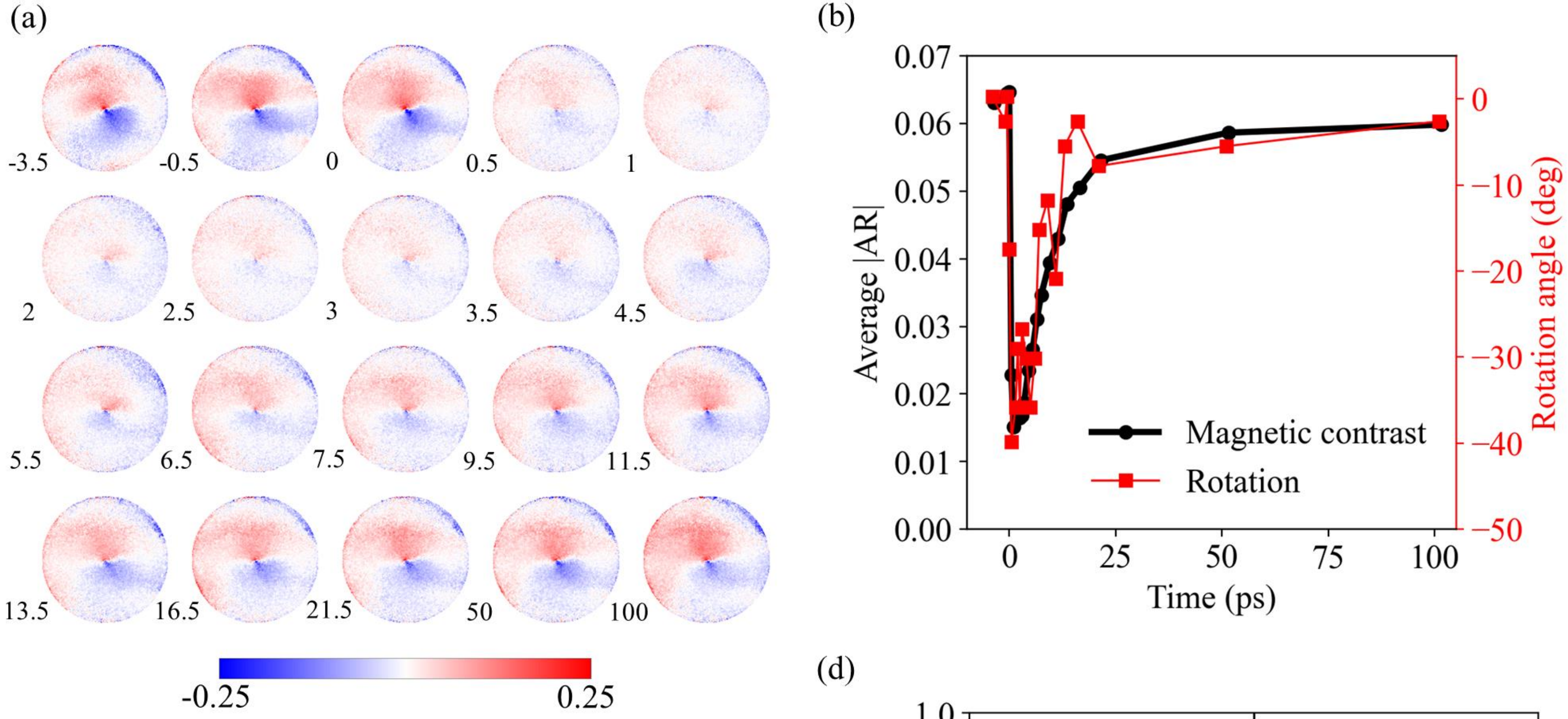

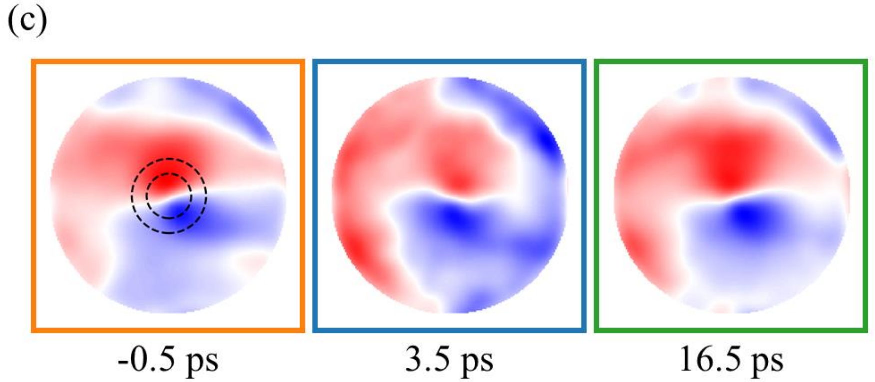

$\ell = -1$

(Fluence F_1)

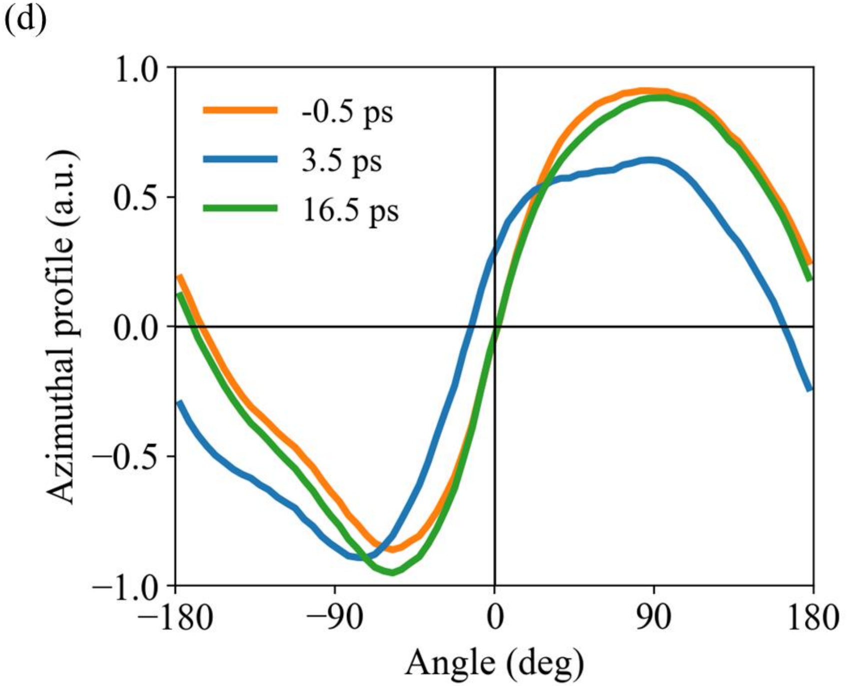

Same time scale!

↓

Qualitative change in magnetic topology

MF et al., PRL 134, 156701 (2025)

tMHD

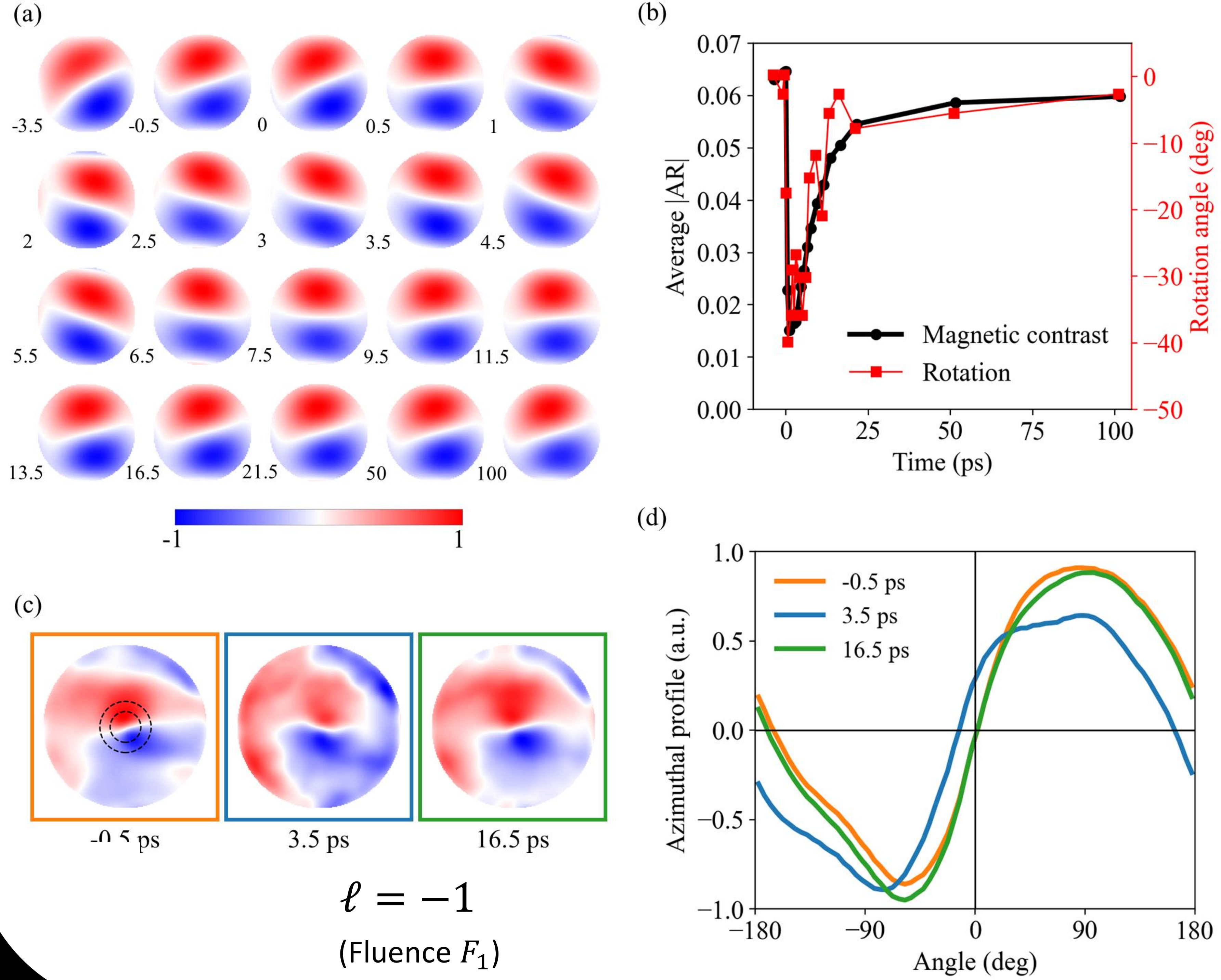

$\ell = -1$

(Fluence F_1)

Same time scale!

Qualitative change in magnetic topology

MF et al., PRL 134, 156701 (2025)

Dependence on OAM and fluence

Max rotation increases with fluence

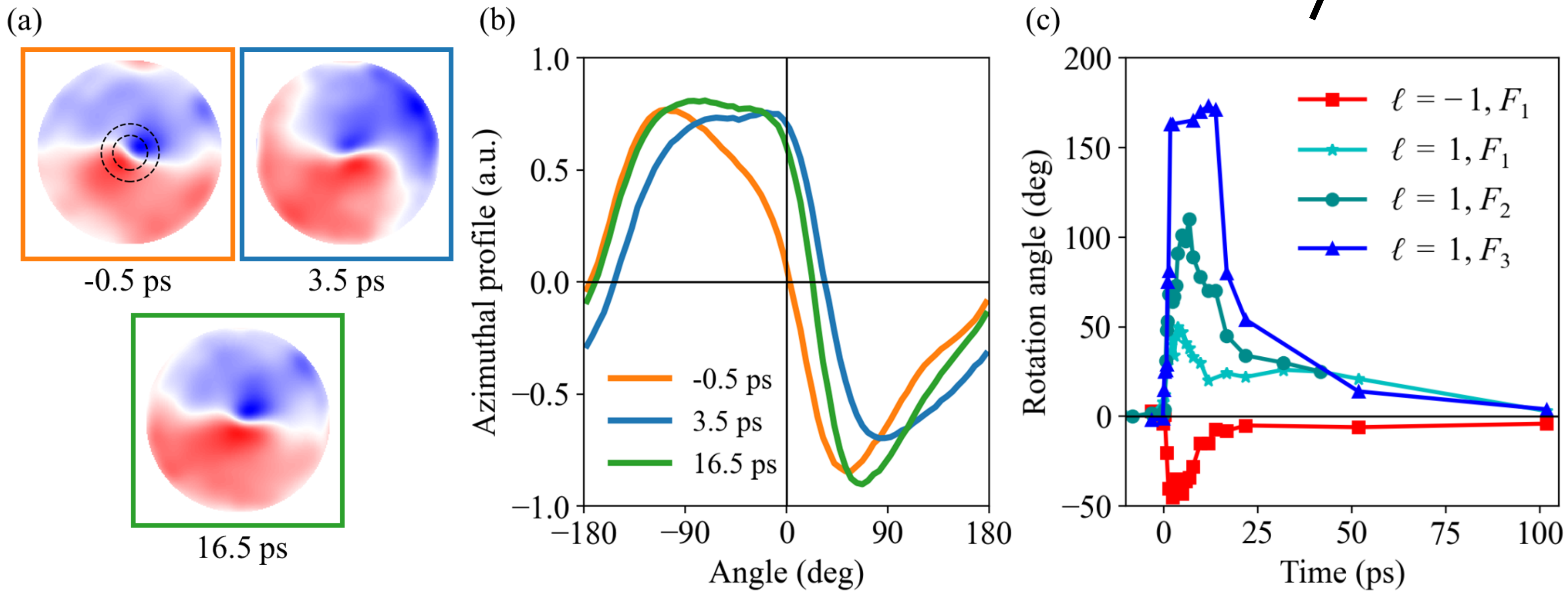

$\ell = +1$

I_1, F_1 : 1.0 μJ/pulse, 4.5 mJ/cm^2

I_2, F_2 :1.4 μJ/pulse, 6.3 mJ/cm^2

I_3, F_3 :1.8 μJ/pulse, 8.1 mJ/cm^2

MF et al., PRL 134, 156701 (2025)

Micromagnetic model

- IR deposits thermal energy → depth and temperature dependent demagnetization (fully demagnetized when T>Tc) at t0

$$f(z) = \begin{cases} 1 & , T_0 + \Delta T_{max} e^{-z^2/\xi^2} > T_C \\ \dfrac{T_0 + \Delta T_{max} e^{-z^2/\xi^2}}{T_C} & , T_0 + \Delta T_{max} e^{-z^2/\xi^2} \le T_C \end{cases}$$

$$\boldsymbol{m}(z) = (1 - f(z))\boldsymbol{m}_{eq}(z) + f(z)\boldsymbol{m}_{rand}$$

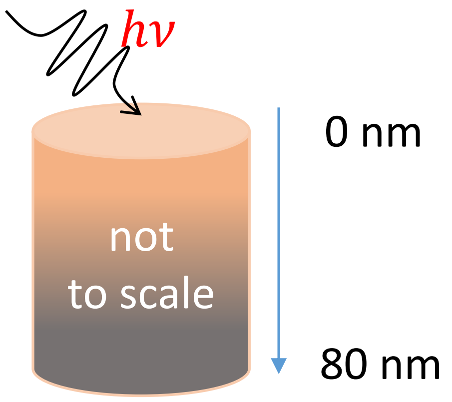

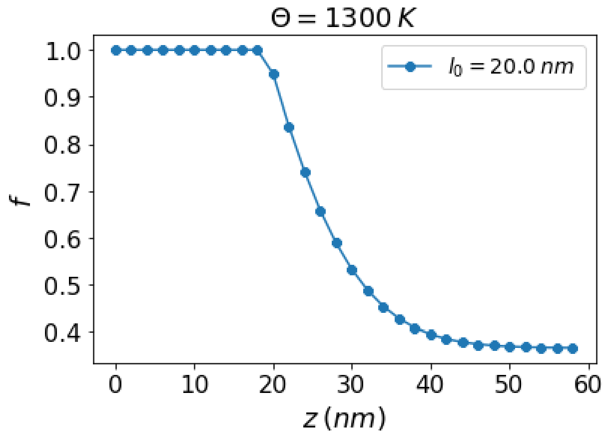

- Let evolve with time → layer dependent magnetization as a function of time

- Input the results into MHD simulations, weighting the near field with the penetration depth

MF et al., PRL 134, 156701 (2025)

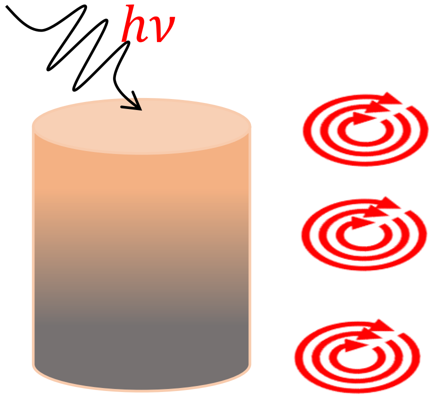
hν

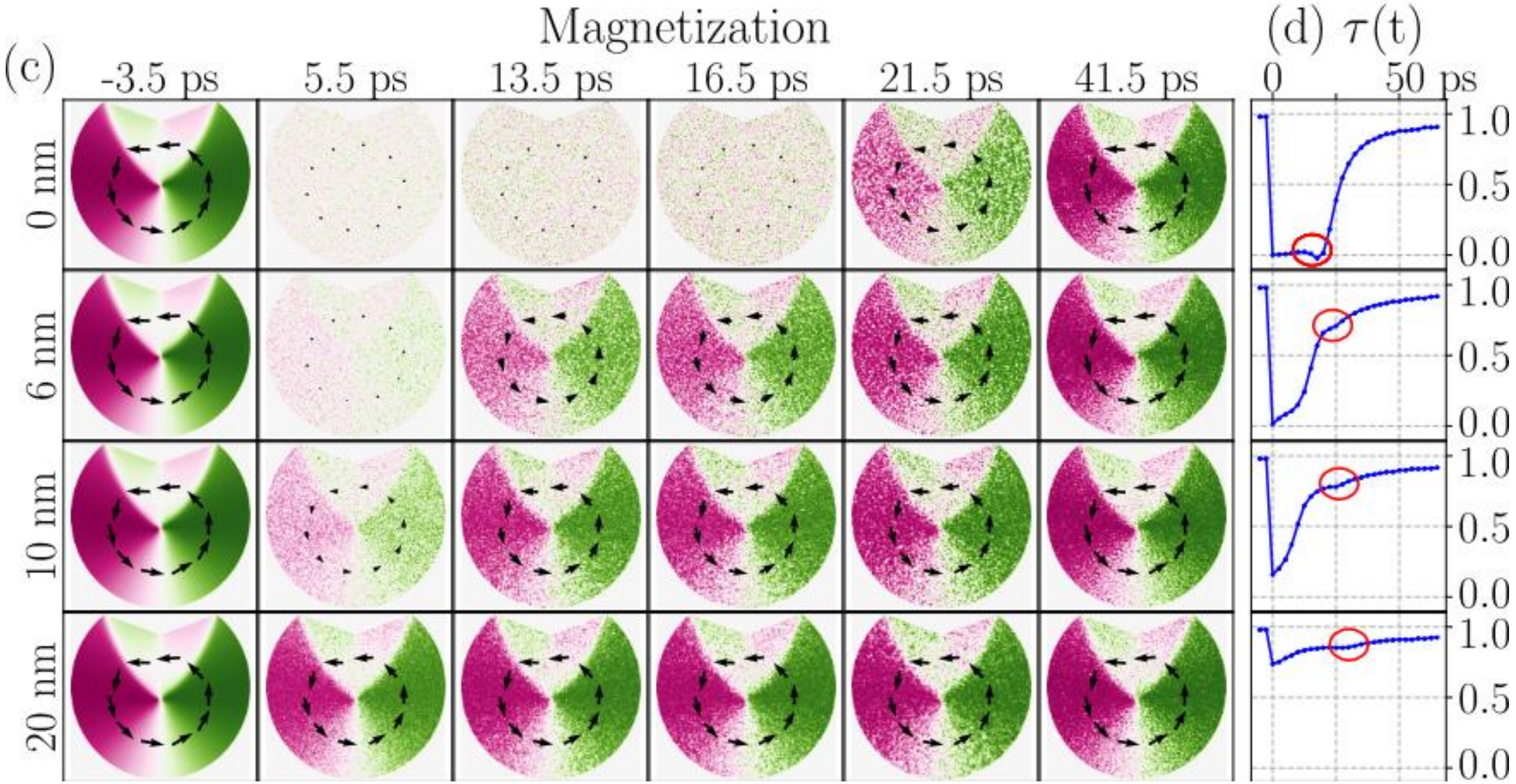
Magnetization
(c)
-3.5 ps
5.5 ps
13.5 ps
16.5 ps
21.5 ps
41.5 ps
0 nm
6 nm
10 nm
20 nm
(d) τ(t)
0
50 ps
1.0
0.5
0.0

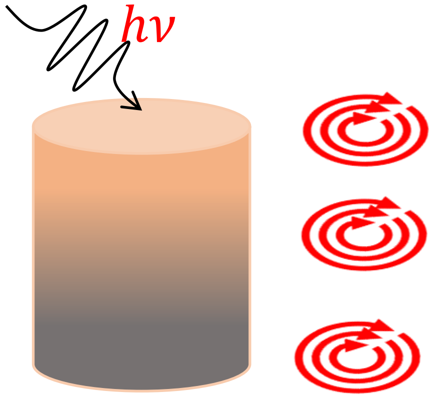
hν

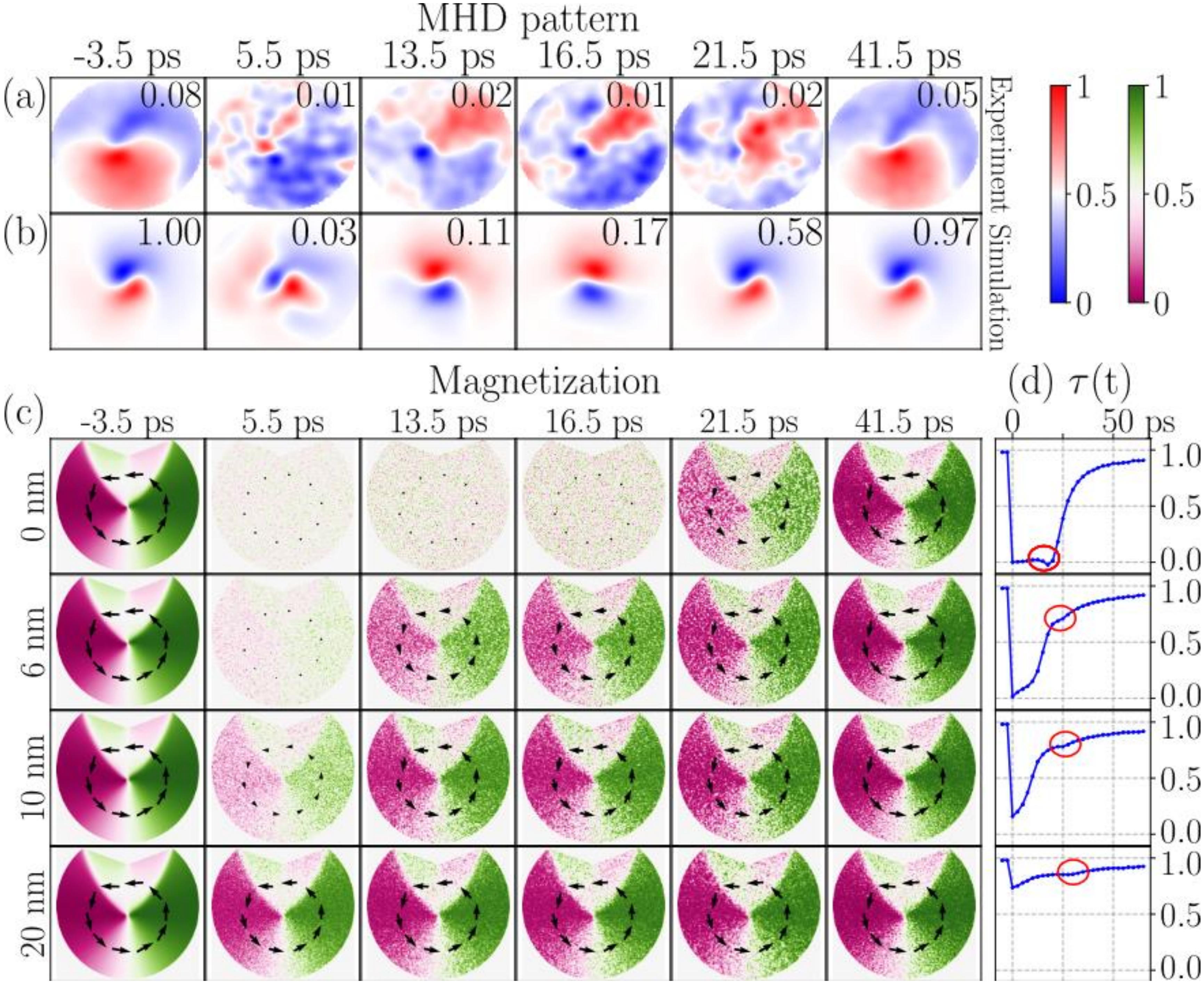
MHD pattern
-3.5 ps
5.5 ps
13.5 ps
16.5 ps
21.5 ps
41.5 ps
(a)
0.08
0.01
0.02
0.01
0.02
0.05
Experiment
(b)
1.00
0.03
0.11
0.17
0.58
0.97
Simulation
1
0.5
0
1
0.5
0
Magnetization
(c)
-3.5 ps
5.5 ps
13.5 ps
16.5 ps
21.5 ps
41.5 ps
0 nm
6 nm
10 nm
20 nm
(d) τ(t)
0
50 ps
1.0
0.5
0.0

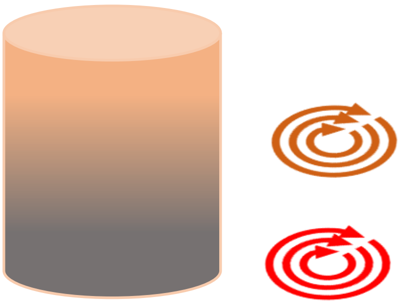

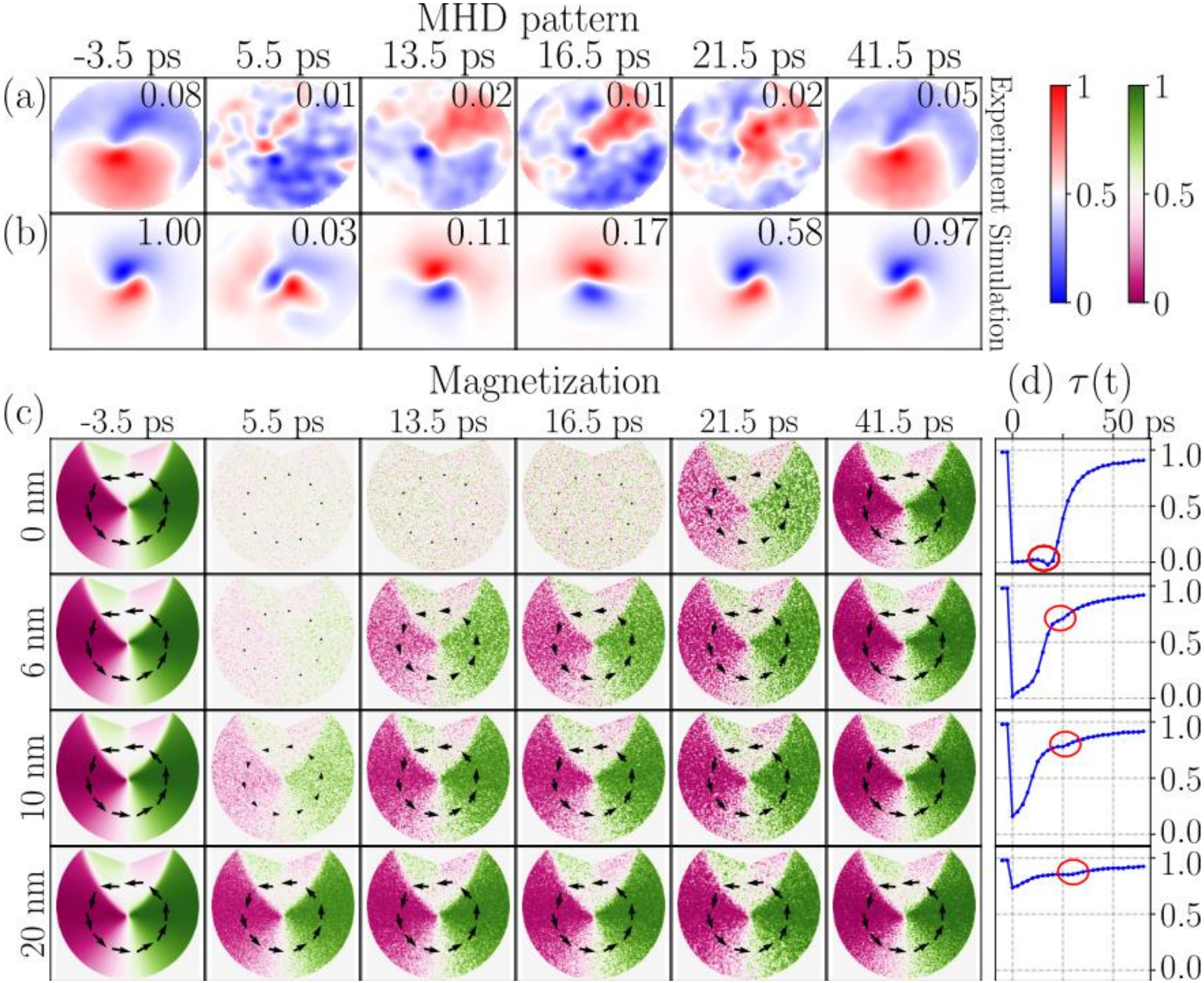

MHD pattern
-3.5 ps
5.5 ps
13.5 ps
16.5 ps
21.5 ps
41.5 ps
(a)
0.08
0.01
0.02
0.01
0.02
0.05
Experiment
(b)
1.00
0.03
0.11
0.17
0.58
0.97
Simulation
1
0.5
0
1
0.5
0
Magnetization
(c)
-3.5 ps
5.5 ps
13.5 ps
16.5 ps
21.5 ps
41.5 ps
0 nm
6 nm
10 nm
20 nm
(d) τ(t)
0
50 ps
1.0
0.5
0.0

Transient reversal of vortex curling!

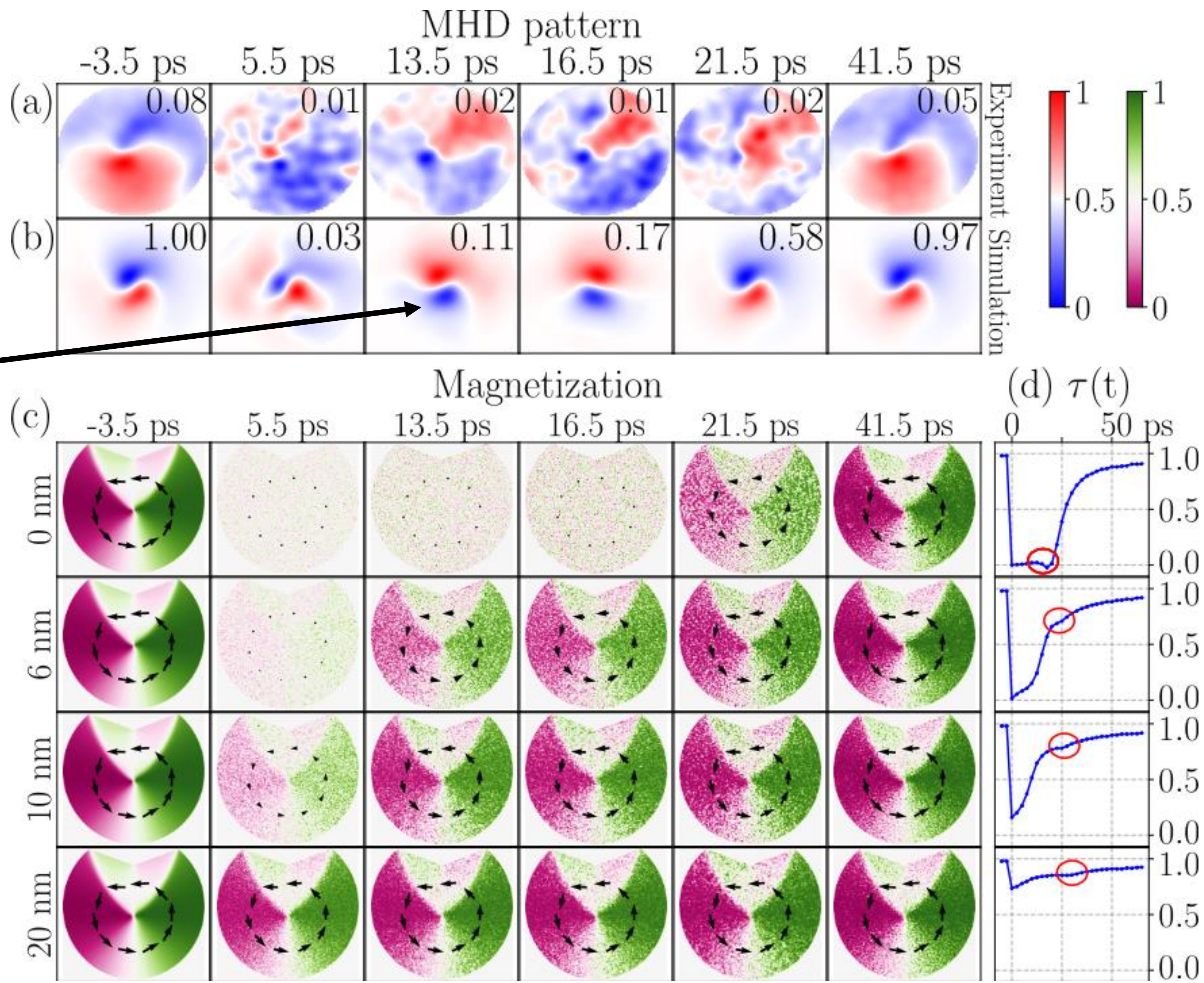

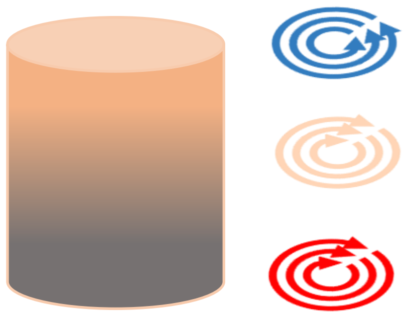

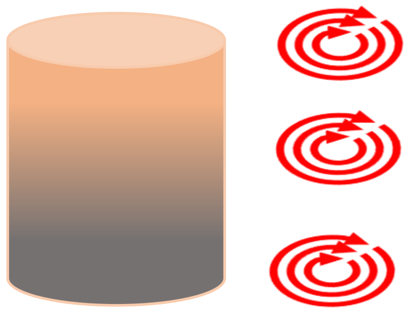

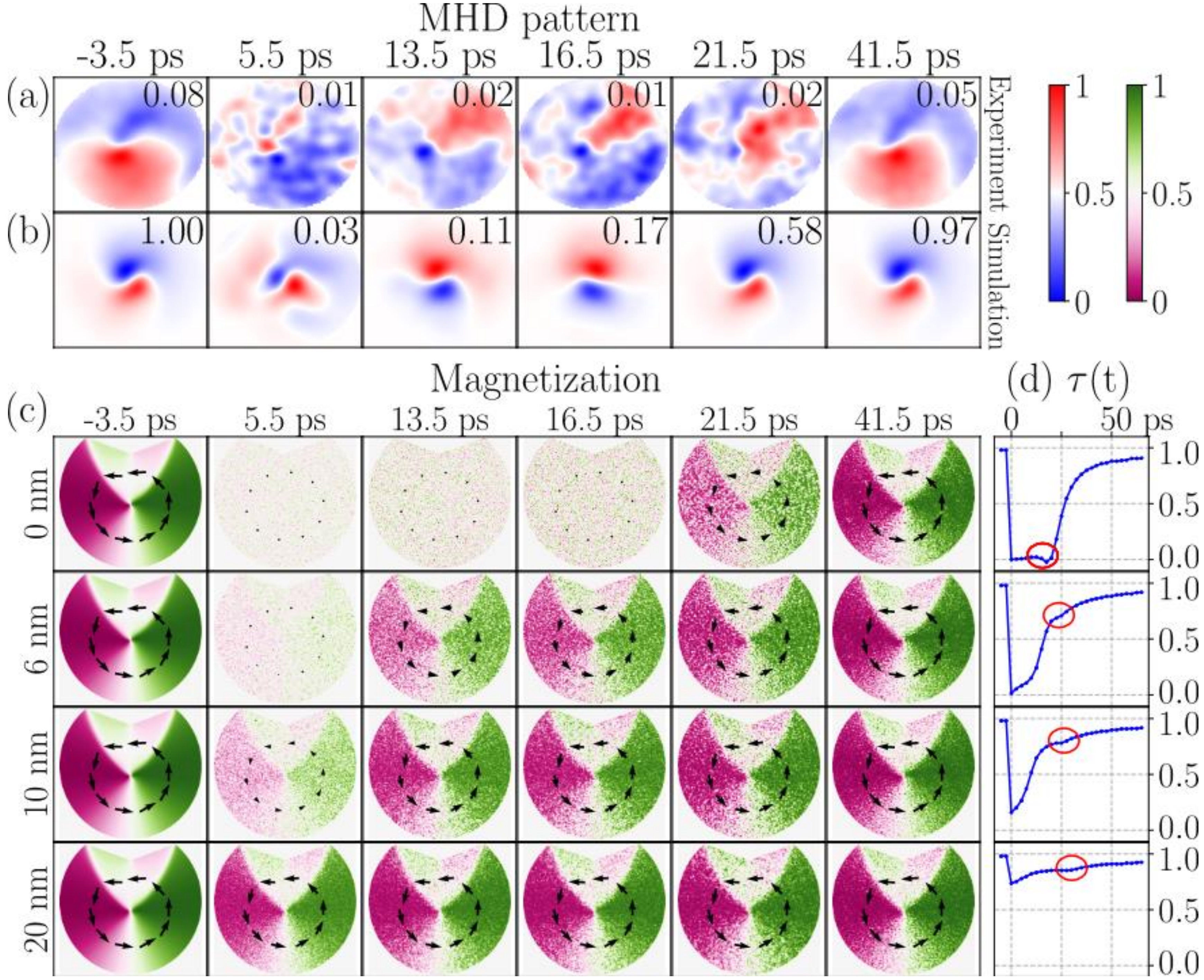
MHD pattern
-3.5 ps
5.5 ps
13.5 ps
16.5 ps
21.5 ps
41.5 ps
(a)
0.08
0.01
0.02
0.01
0.02
0.05
Experiment
(b)
1.00
0.03
0.11
0.17
0.58
0.97
Simulation
1
0.5
0
1
0.5
0
Magnetization
(c)
-3.5 ps
5.5 ps
13.5 ps
16.5 ps
21.5 ps
41.5 ps
0 nm
6 nm
10 nm
20 nm
(d) $\tau(t)$
0
50 ps
1.0
0.5
0.0

Toroidal moment $\propto$ <u>Vortex toroidicity</u> $\tau = \int_0^{2\pi} \hat{u}_m(\theta, t) \cdot \hat{u}_\theta \, d\theta$

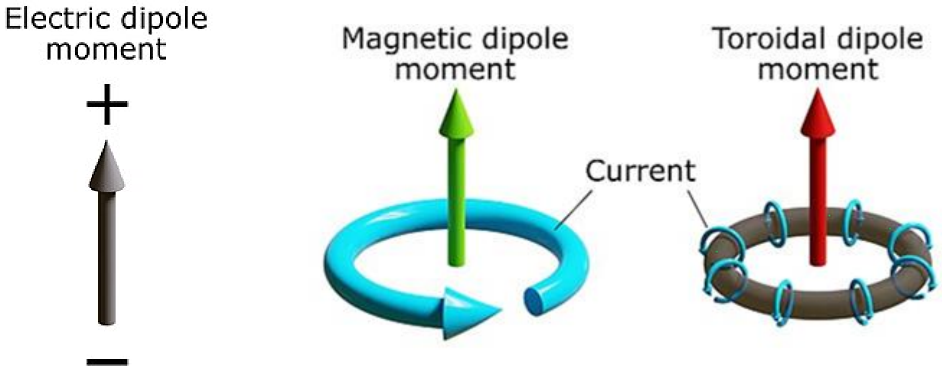

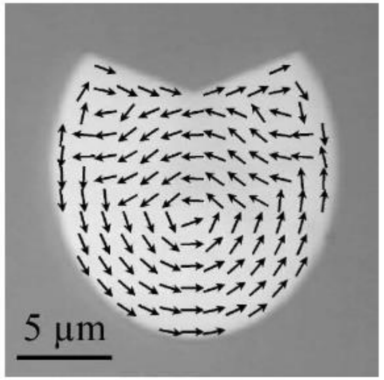

MF et al., PRL 134, 156701 (2025)

Toroidal moment ∝ Vortex toroidicity $\tau = \int_0^{2\pi} \hat{u}_m(\theta, t) \cdot \hat{u}_\theta d\theta$

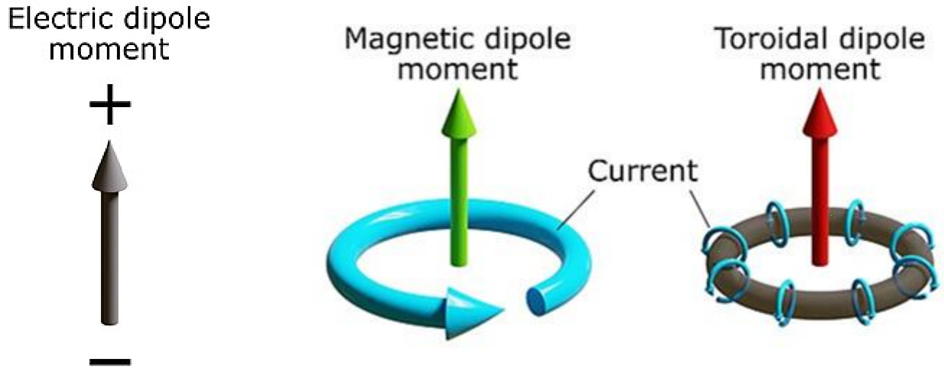

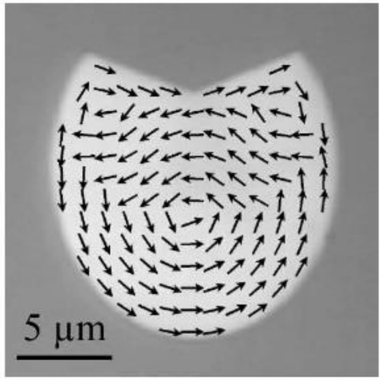

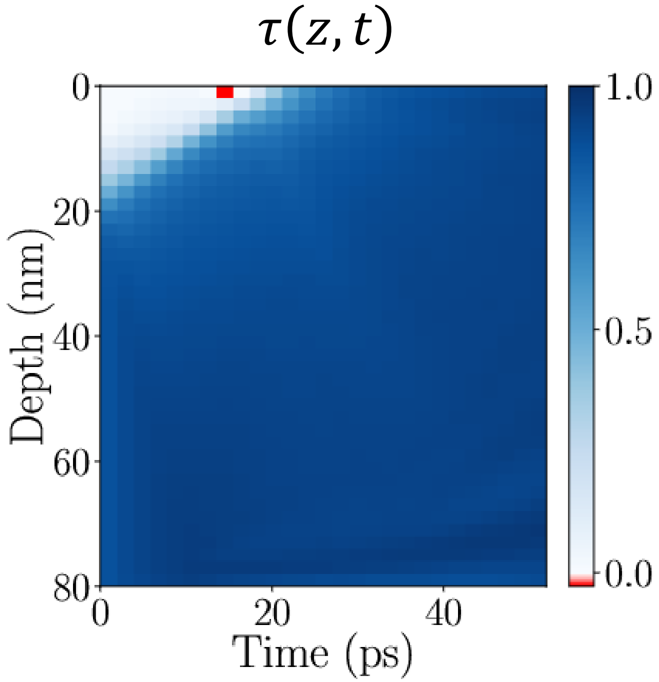

MF et al., PRL 134, 156701 (2025)

Toroidal moment ∝ <u>Vortex toroidicity</u> $\tau = \int_0^{2\pi} \hat{u}_m(\theta, t) \cdot \hat{u}_\theta d\theta$

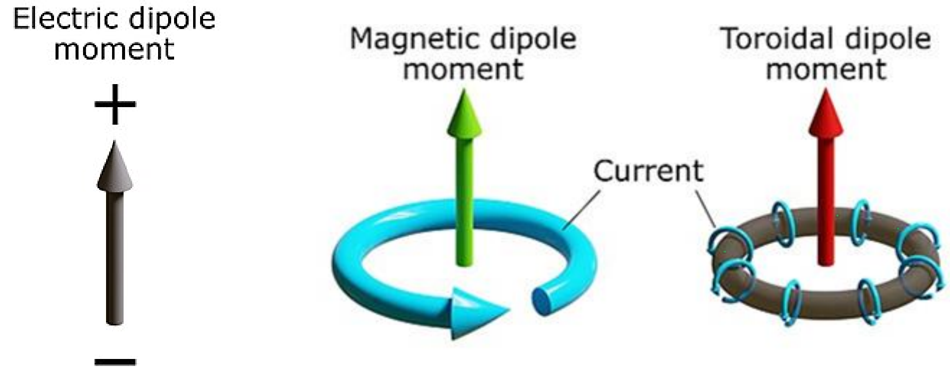

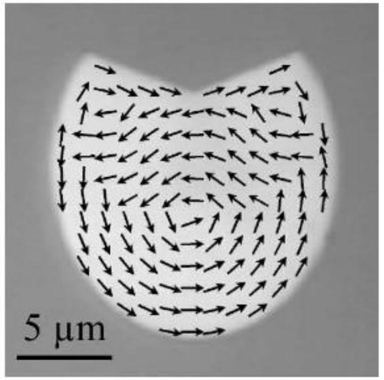

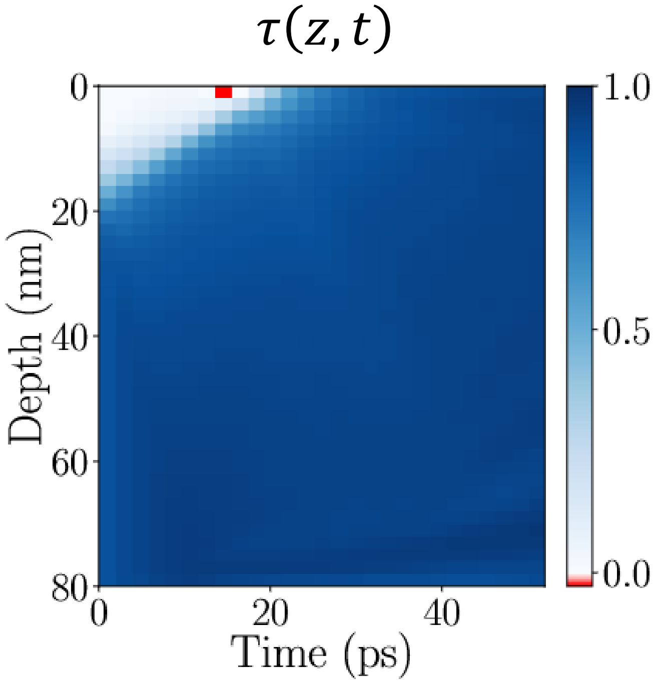

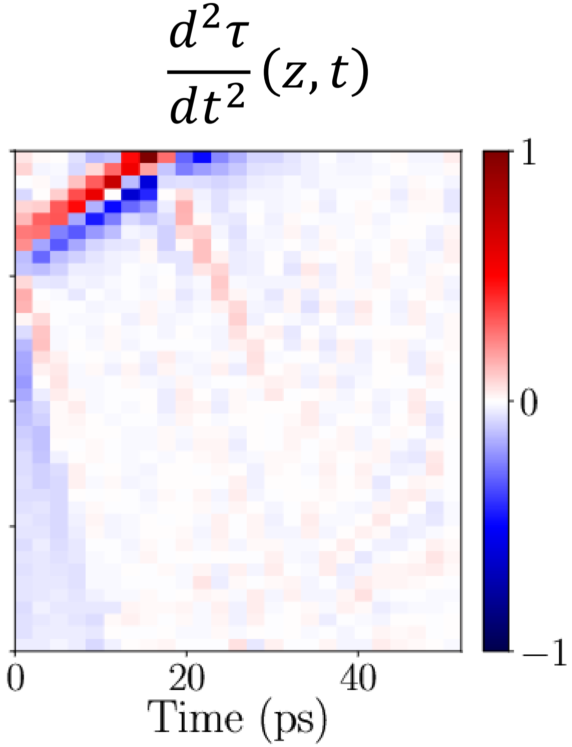

Phonon velocity: $\sim 3 \cdot 10^3 m/s$

MF et al., PRL 134, 156701 (2025)

Conclusions and perspectives

Conclusions

- Similar to **magnetic circular dichroism** (MCD), obtained when switching the **spin** angular momentum of the photon, **magnetic helicoidal dichroism** (MHD) is obtained when switching its **orbital** angular momentum

Conclusions

- Similar to **magnetic circular dichroism** (MCD), obtained when switching the **spin** angular momentum of the photon, **magnetic helicoidal dichroism** (MHD) is obtained when switching its **orbital** angular momentum

  ✓ Development of classical electromagnetic **theory** for **MHD** in **resonant magnetic scattering**

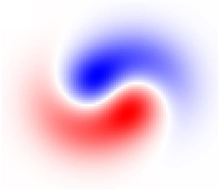

PRA 103, 013501 (2021)

Conclusions

- Similar to **magnetic circular dichroism** (MCD), obtained when switching the **spin** angular momentum of the photon, **magnetic helicoidal dichroism** (MHD) is obtained when switching its **orbital** angular momentum

  - ✓ Development of classical electromagnetic **theory** for **MHD** in **resonant magnetic scattering**

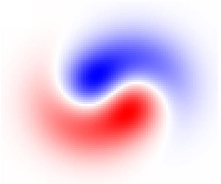

PRA 103, 013501 (2021)

  - ✓ Good match with **experimental findings**, showing the potential of MHD as a **new investigation tool** for **ultrafast** magnetization dynamics with topology resolution

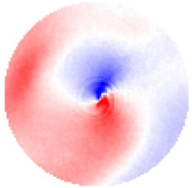

PRL 128, 077401 (2022)

Conclusions

- Similar to **magnetic circular dichroism** (MCD), obtained when switching the **spin** angular momentum of the photon, **magnetic helicoidal dichroism** (MHD) is obtained when switching its **orbital** angular momentum

✓ Development of classical electromagnetic **theory** for **MHD** in **resonant magnetic scattering**

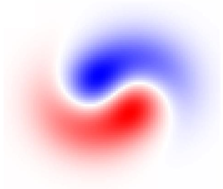

PRA 103, 013501 (2021)

✓ Good match with **experimental findings**, showing the potential of MHD as a **new investigation tool** for **ultrafast** magnetization dynamics with topology resolution

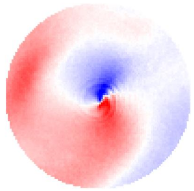

PRL 128, 077401 (2022)

✓ Observed **transient reversal of magnetic vortex curling** on a 20 ps time scale upon **ultrafast optical pumping**

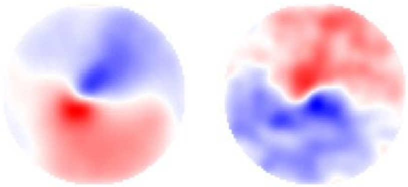

PRL 134, 156701 (2025)

Perspectives

- <u>Fundamental understandings</u>

- <u>Using OAM beams in other experiments</u>

Perspectives

- **Fundamental understandings**
  - Photon spin-orbit coupling
  - Transfer of angular momentum

Talk by M. Luttmann

- **Using OAM beams in other experiments**

Change in OAM upon magnetic reflection is governed by the SAM of the incident field

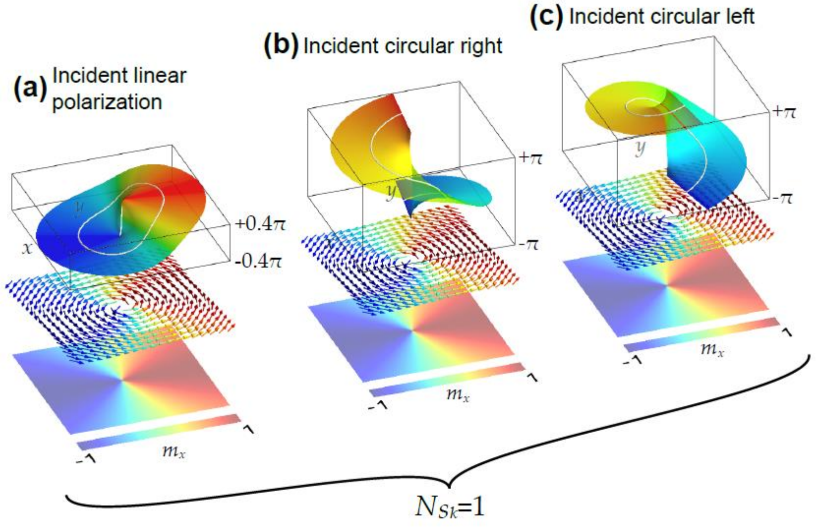

M. Luttmann et al., submitted

Perspectives

- <u>Fundamental understandings</u>
  - Photon spin-orbit coupling
  - Transfer of angular momentum
  - Another point of view for well-know magneto-optic effects
- <u>Using OAM beams in other experiments</u>

Redistribution of OAM modes upon magnetic scattering

$$\forall \ell_{in} : \textit{also for } \ell_{in} = 0 \; (!!!)$$

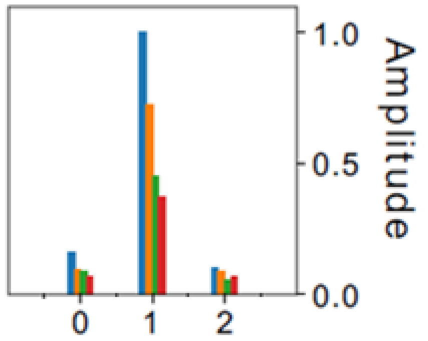

Perspectives

- Fundamental understandings
  - Photon spin-orbit coupling
  - Transfer of angular momentum
  - Microscopic theory?
- Using OAM beams in other experiments
  - Pthychography

Talk by G. F. Mancini

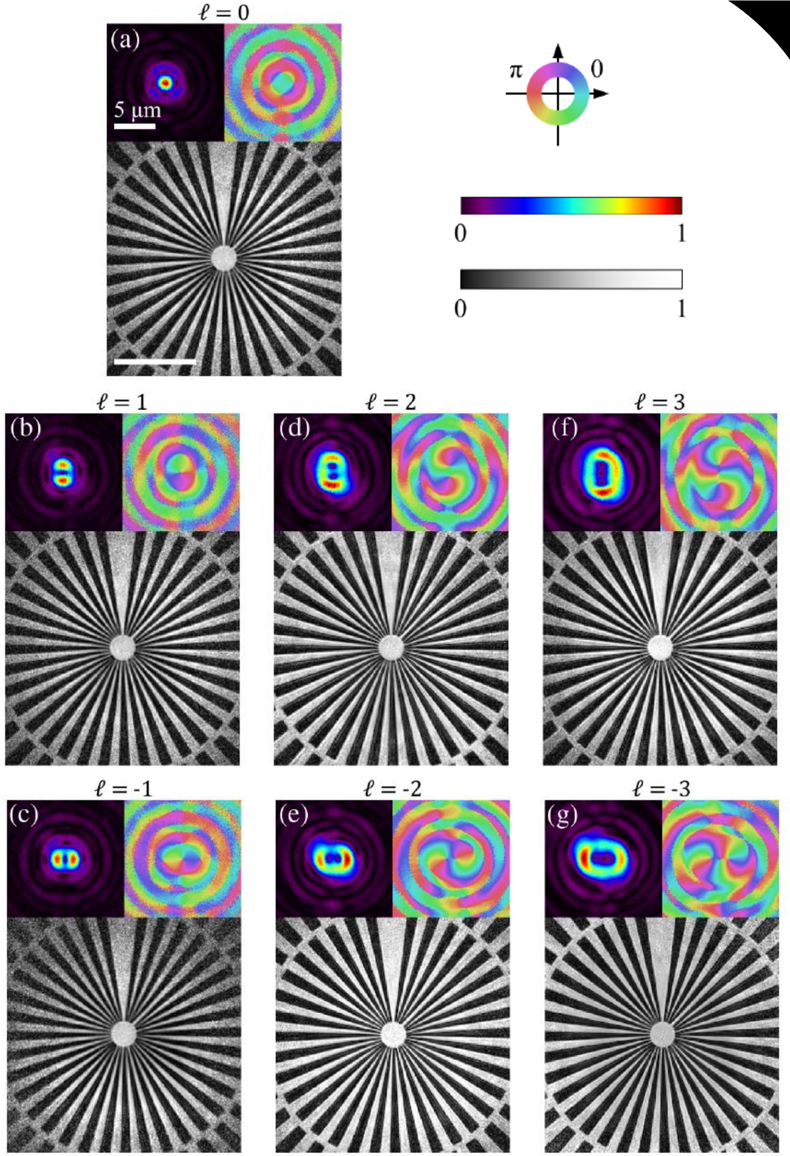

M. Pancaldi et al., Optica 11, 3, 403 (2024)

- Spatial resolution increases with OAM
- Very sensitive to optical aberrations
- T-resolved imaging of plasmons and phonons

Perspectives

- Fundamental understandings
  - Photon spin-orbit coupling
  - Transfer of angular momentum
  - Microscopic theory?
- Using OAM beams in other experiments
  - Pthychography
  - X-ray spectroscopies (XAS, RIXS…)

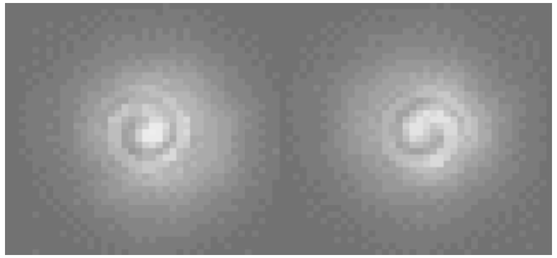

Talk by M. Sacchi

Perspectives

- Fundamental understandings
  - Photon spin-orbit coupling
  - Transfer of angular momentum
  - Microscopic theory?
- Using OAM beams in other experiments
  - Pthychography
  - X-ray spectroscopies (XAS, RIXS…)
  - Photoemission spectroscopy

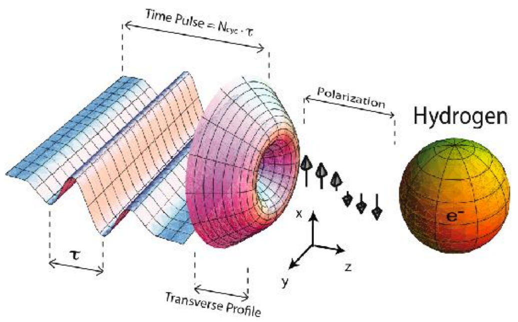

A. Picón et al., Opt. Express 18, 3660 (2010)

G. De Ninno et al., Nat. Phot. 14, 554 (2020)

- Selection rules: $|\Delta L| = 1 \rightarrow |\Delta L| \leq |l| + 1$
- Dipole/quadrupole
- Interplay SAM and OAM of photons and electrons
- OAM in pump/probe
- Transfer to low energy excitations

Perspectives

- Fundamental understandings
  - Photon spin-orbit coupling
  - Transfer of angular momentum
  - Microscopic theory?
- Using OAM beams in other experiments
  - Pthychography
  - X-ray spectroscopies (XAS, RIXS…)
  - Photoemission spectroscopy

CERGY PARIS UNIVERSITÉ

UNIVERSITY OF WEST BOHEMIA

cea PARIS-SACLAY

SUPPLEMENTARY
MHD theory

$\ell_{out} = \ell_{in} + n$

Homogeneous structure:
$n = 0$

$\ell_{in} = 1 = \ell_{out}$

Geometrical effect

$\Delta\ell$ even

Magnetic domain:
$n \in N_{odd}$

$\ell_{in} = 1$
$\ell_{out} = \ell_{in} + n$

Real experiment on inhomogeneous structure

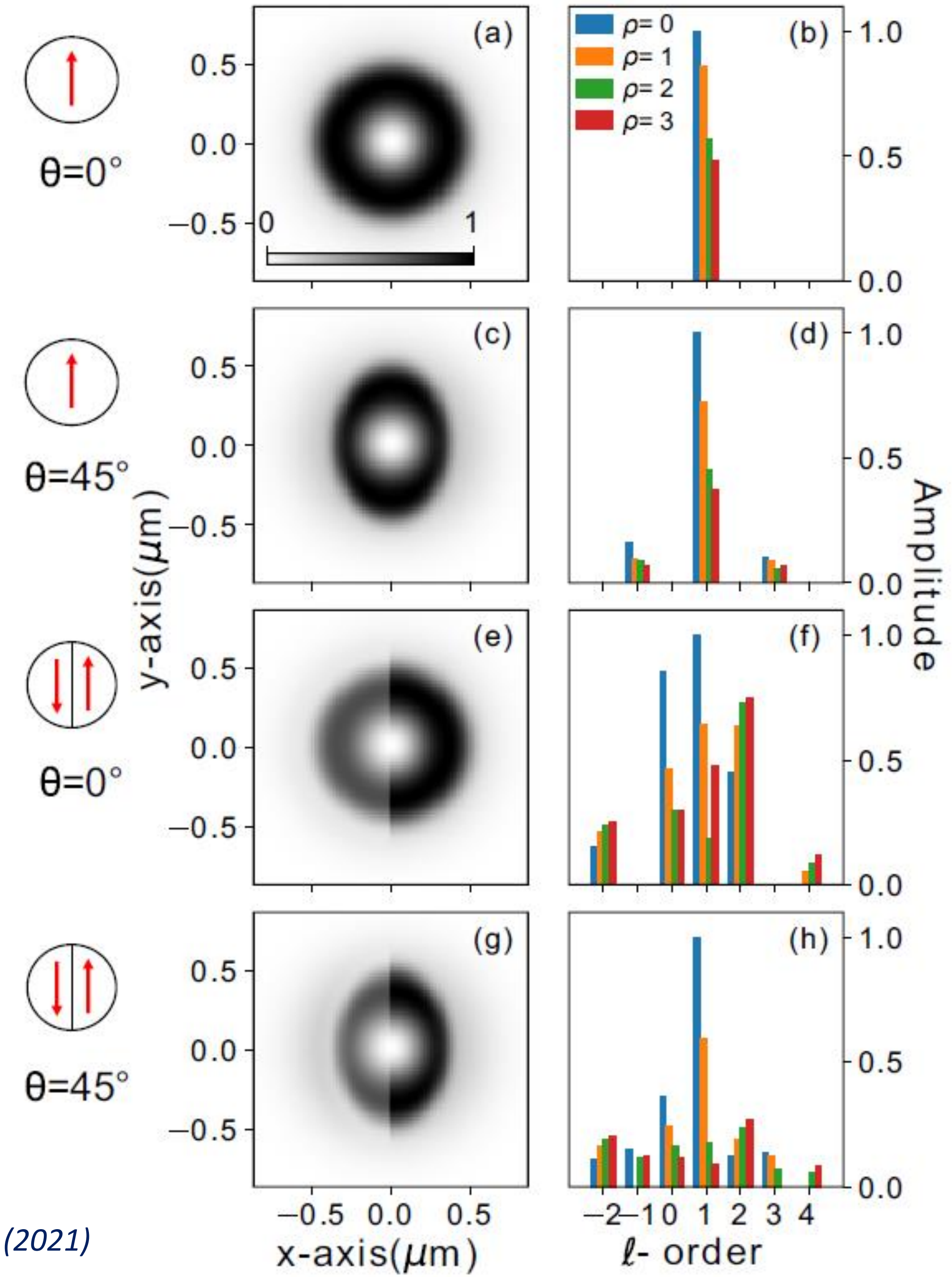

Complicated mode redistribution

A **vortex** is easier since $n = \pm 1$

M. Fanciulli et al., PRA 103, 013501 (2021)

SUPPLEMENTARY
MHD static

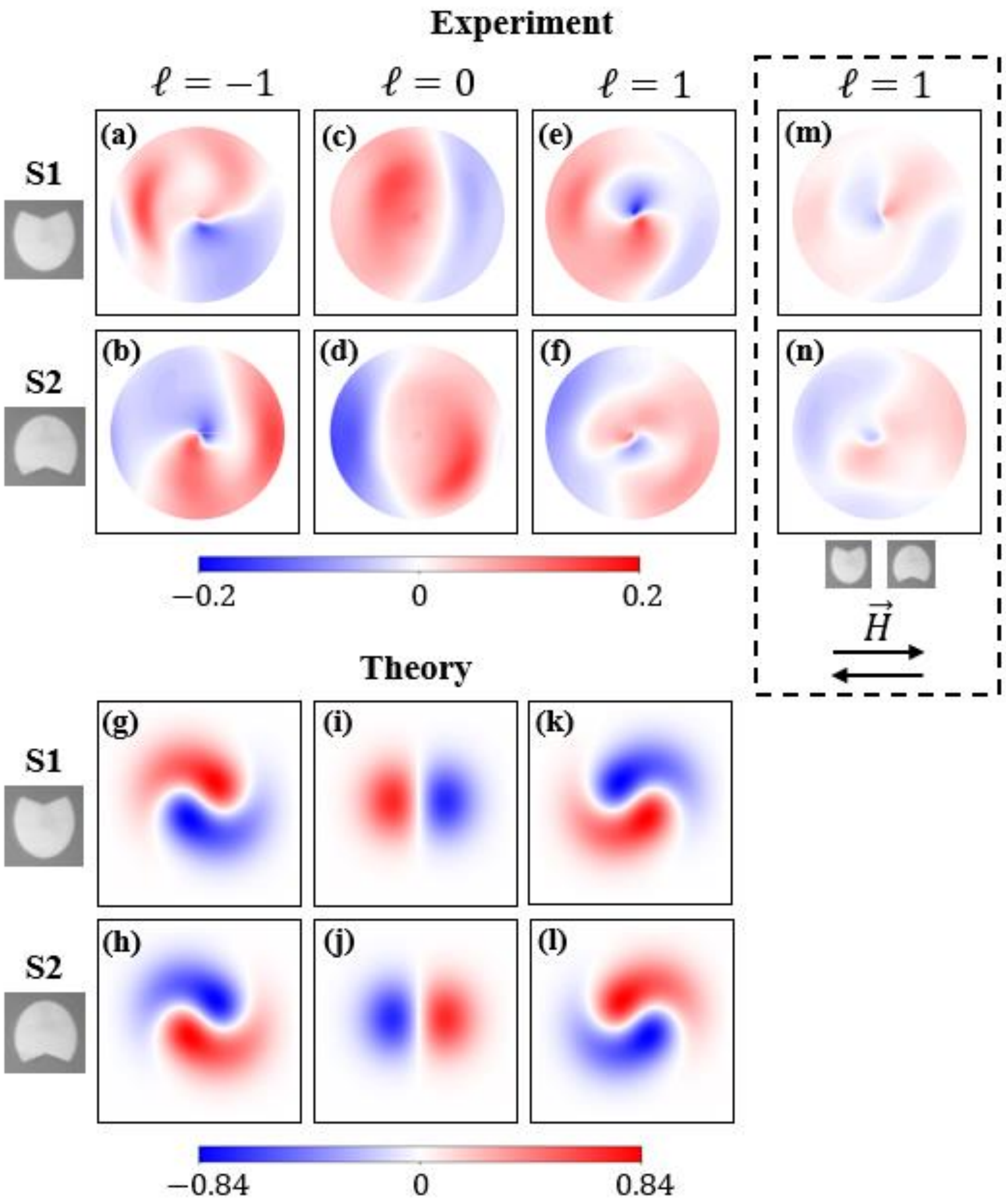

M. Fanciulli et al., PRL 128, 077401 (2022)

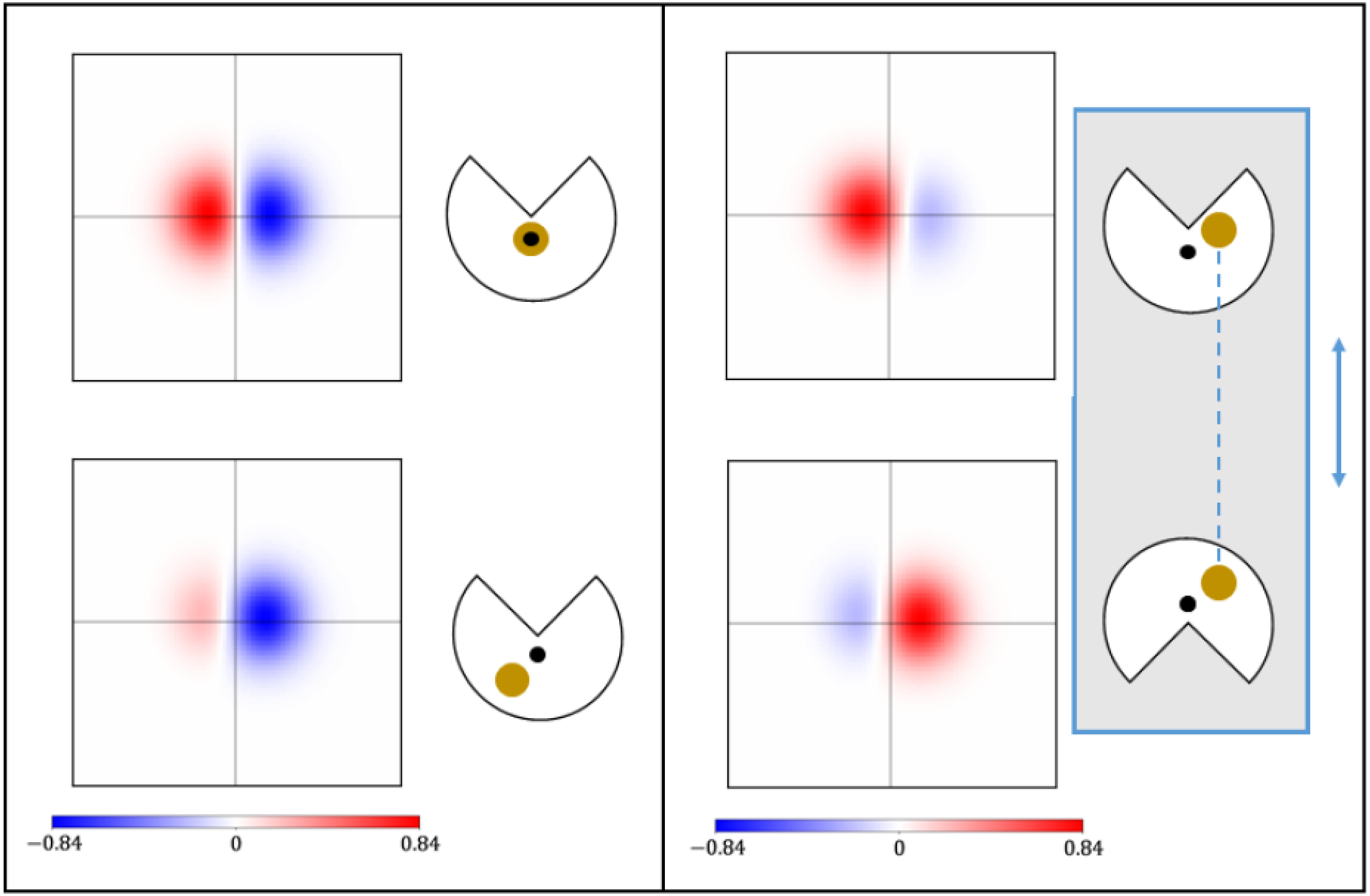

M. Fanciulli et al., PRL 128, 077401 (2022)

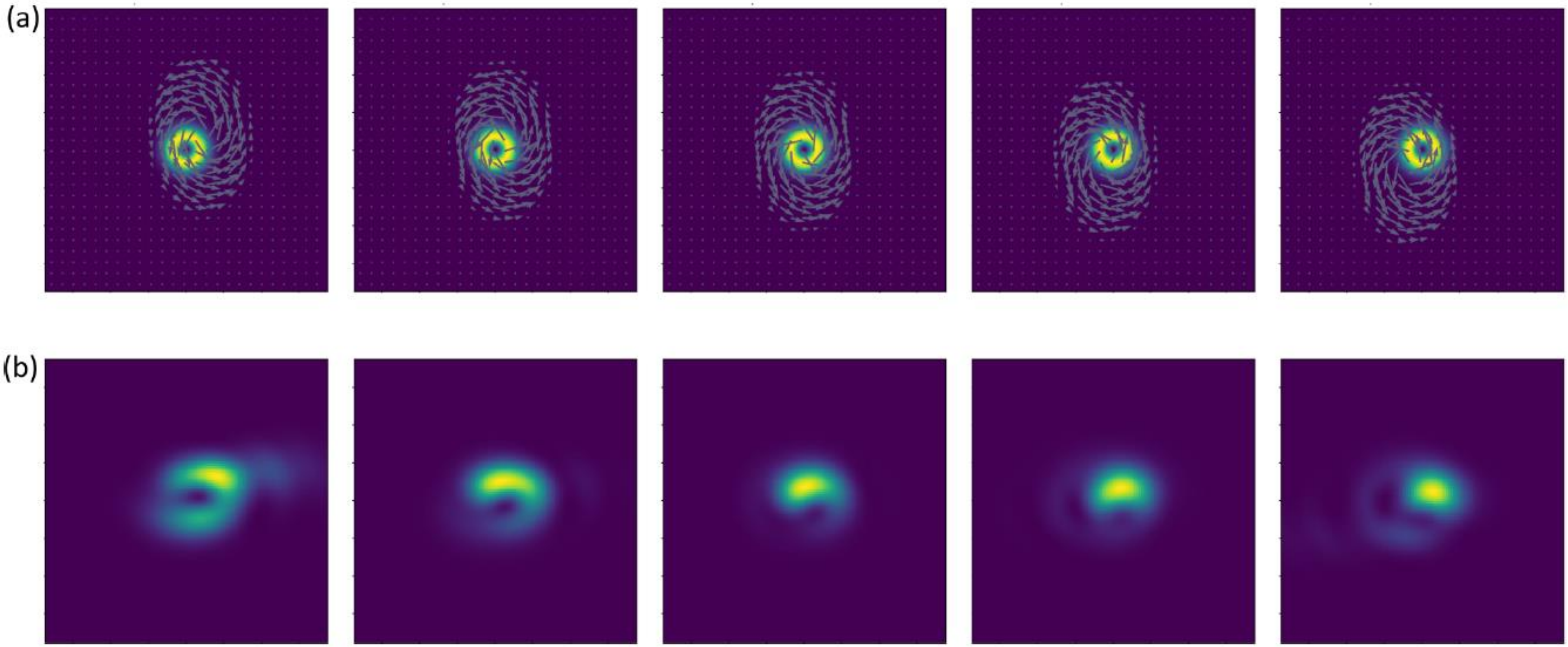

FIG. 7. (a) Numerical simulation of the relative position of an incident beam and a magnetic vortex (diameter of 10 μm and placed at $\theta = 48^\circ$ for this simulation on a square of 17.2 μm) and (b) the resulting reflected intensity in the far field (at 10 cm from the sample here, square of 15 cm).

M. Fanciulli et al., PRA 103, 013501 (2021)

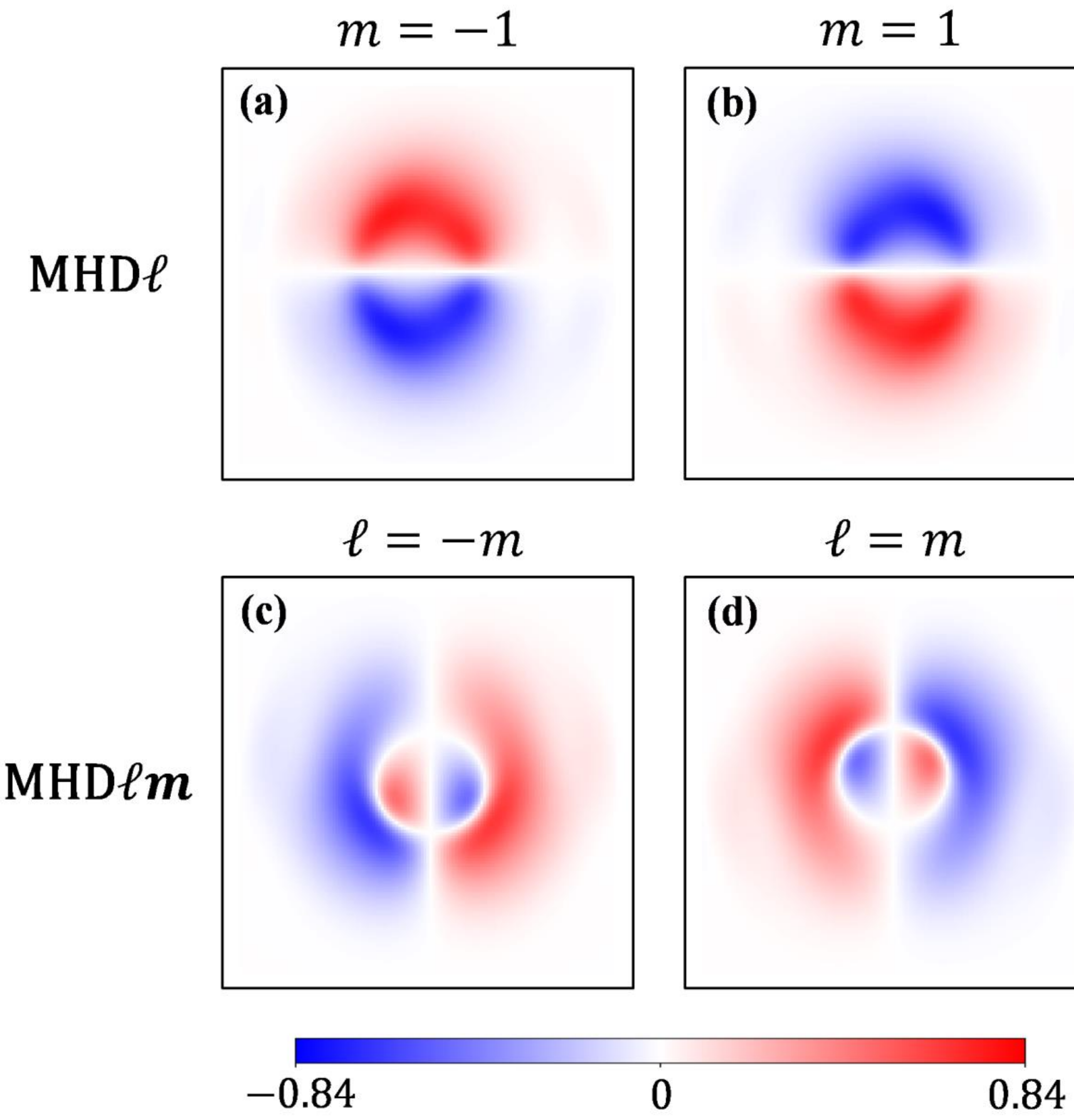

M. Fanciulli et al., PRL 128, 077401 (2022)

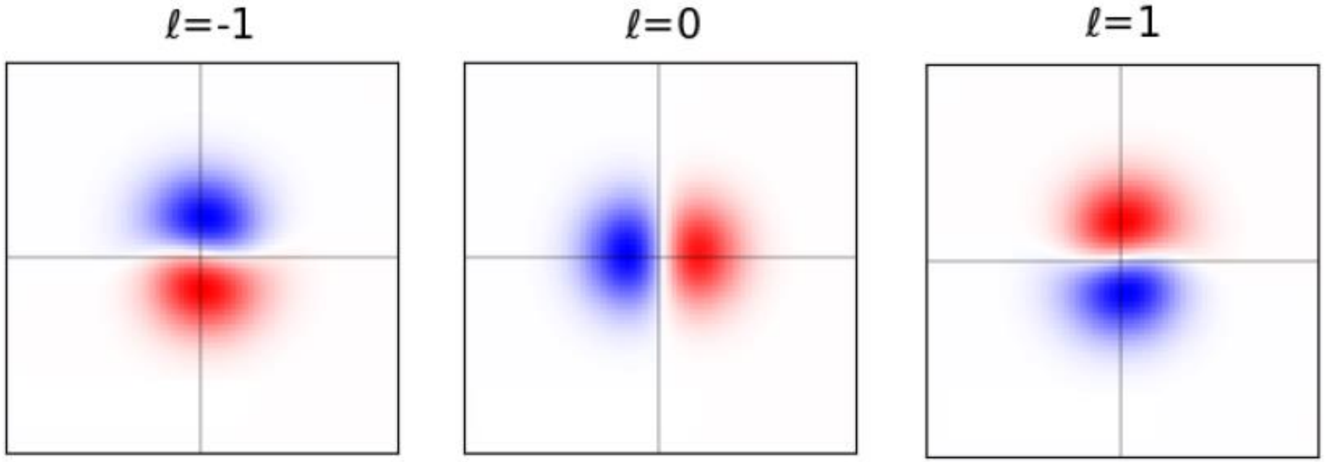

FIG. S5: MHDm calculated for similar conditions as in Fig. 2(g)-(l) of the main text, but for an incidence angle of 5° from the normal. The color scale maximum is 0.65 for $\ell = \pm 1$ and 0.1 for $\ell = 0$.

M. Fanciulli et al., PRL 128, 077401 (2022)

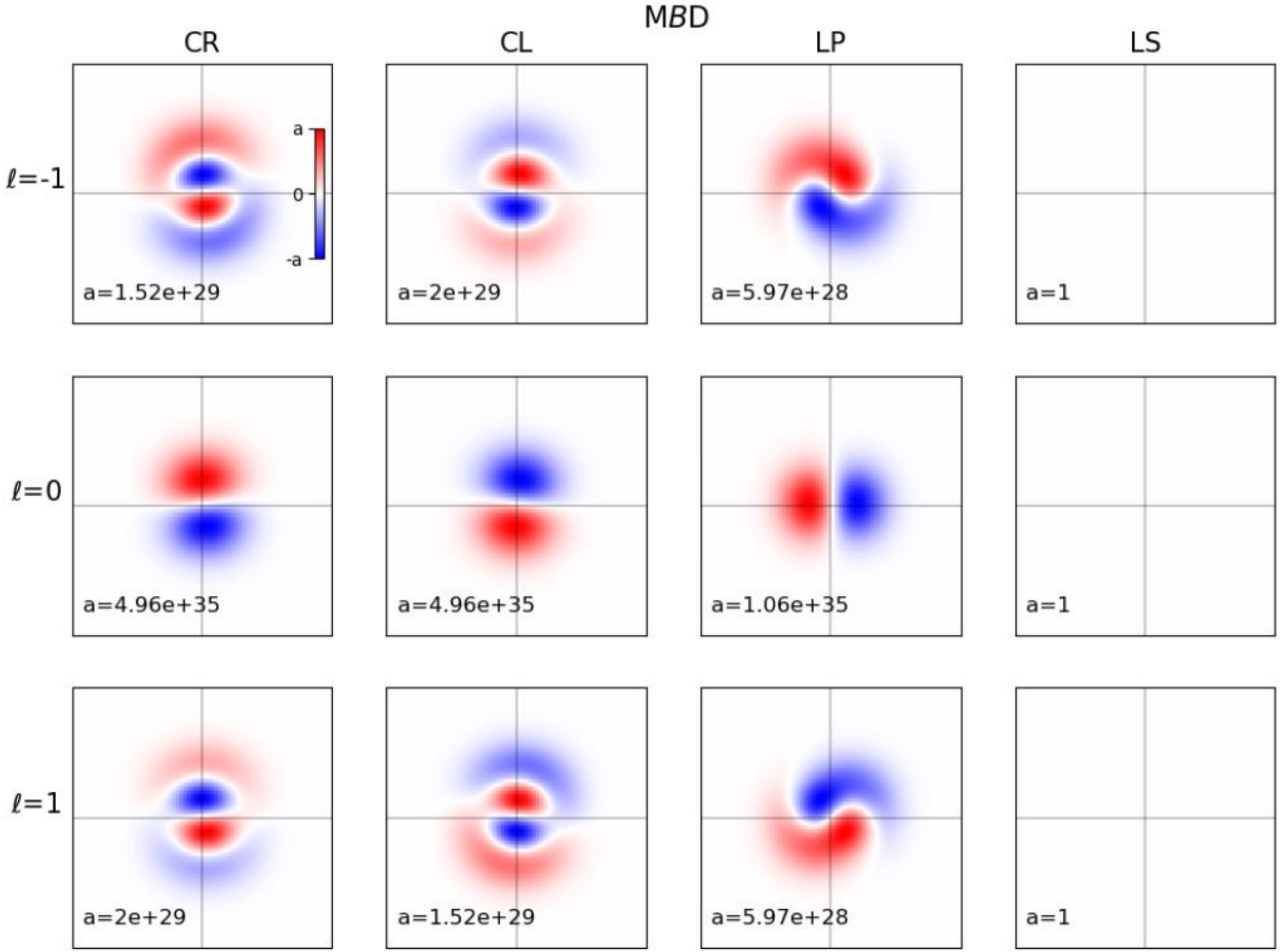

M. Fanciulli et al., PRL 128, 077401 (2022)

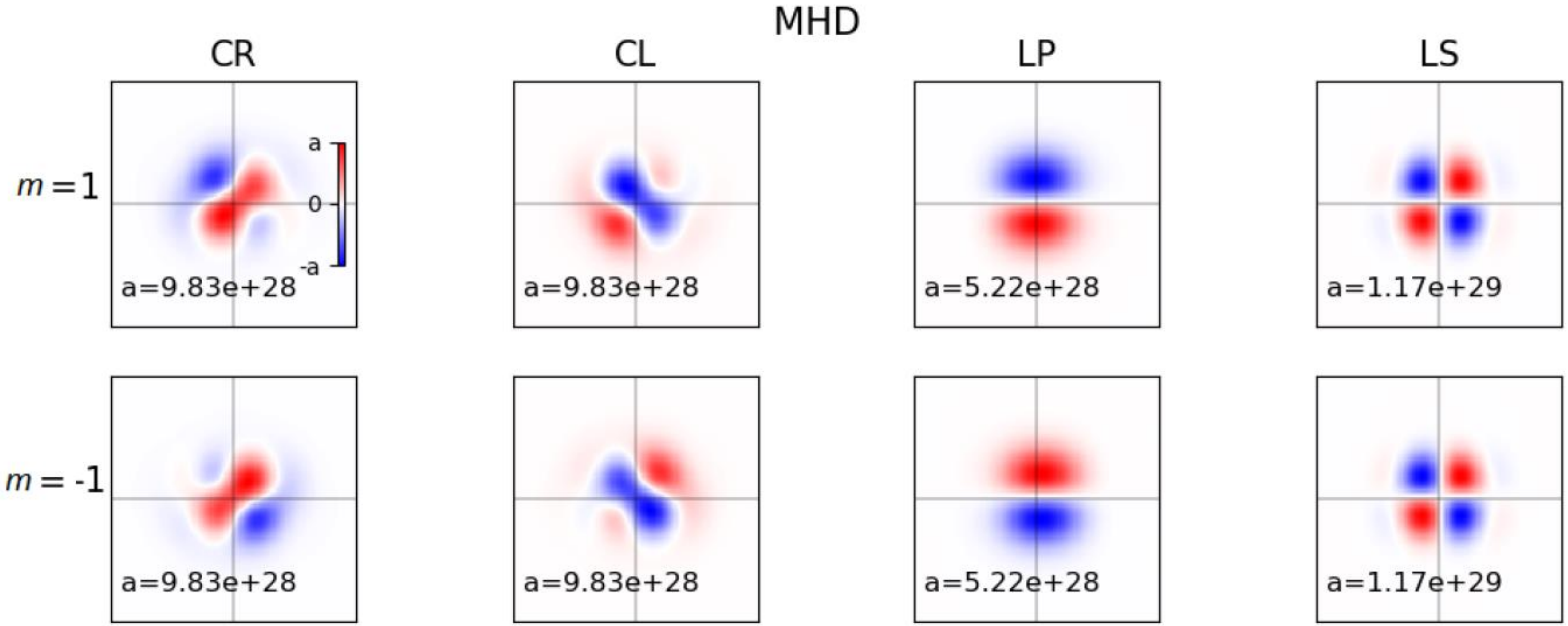

M. Fanciulli et al., PRL 128, 077401 (2022)

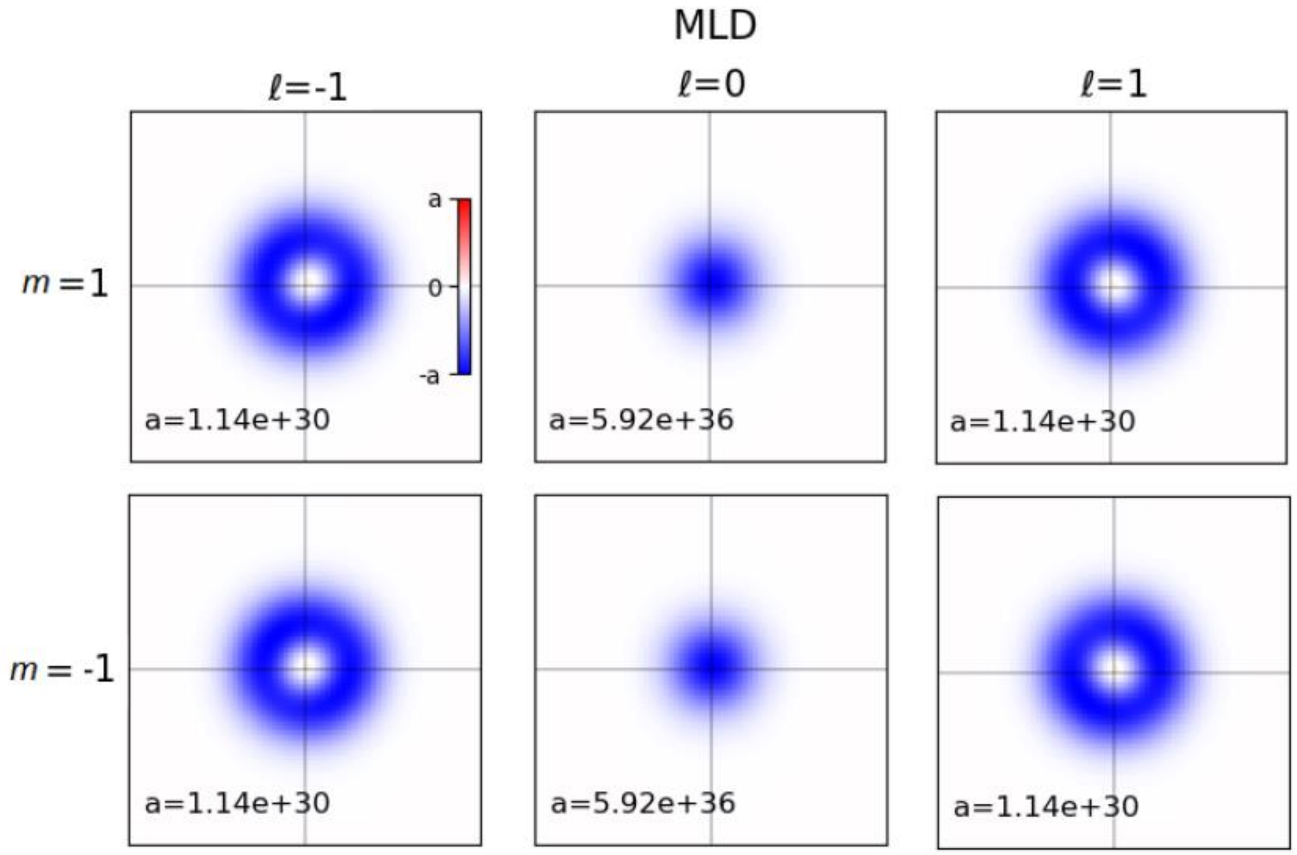

M. Fanciulli et al., PRL 128, 077401 (2022)

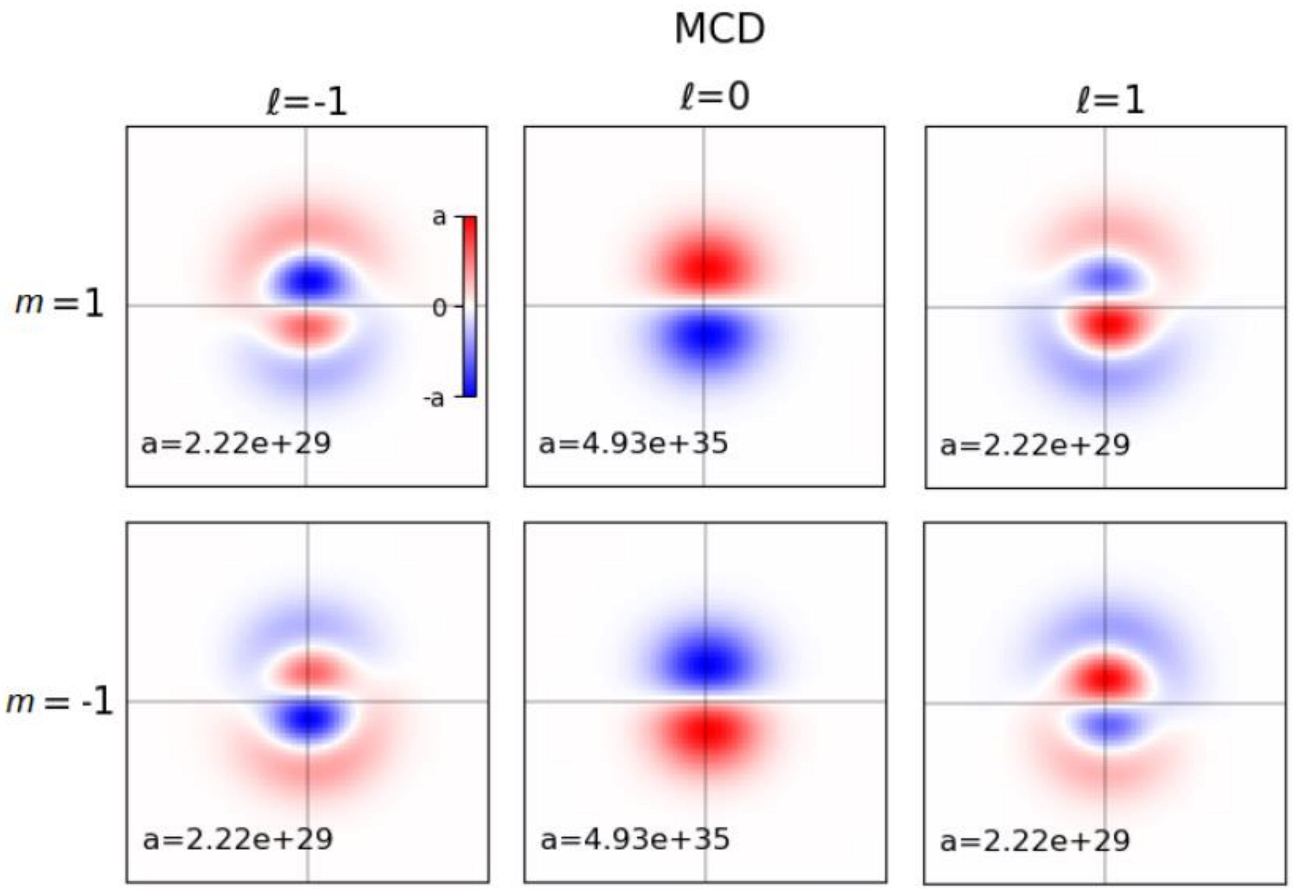

M. Fanciulli et al., PRL 128, 077401 (2022)

SUPPLEMENTARY
tMHD

I_1, F_1 : 1.0 μJ/pulse, 4.5 mJ/cm²

$\ell = +1$

I_3, F_3 :1.8 μJ/pulse, 8.1 mJ/cm²

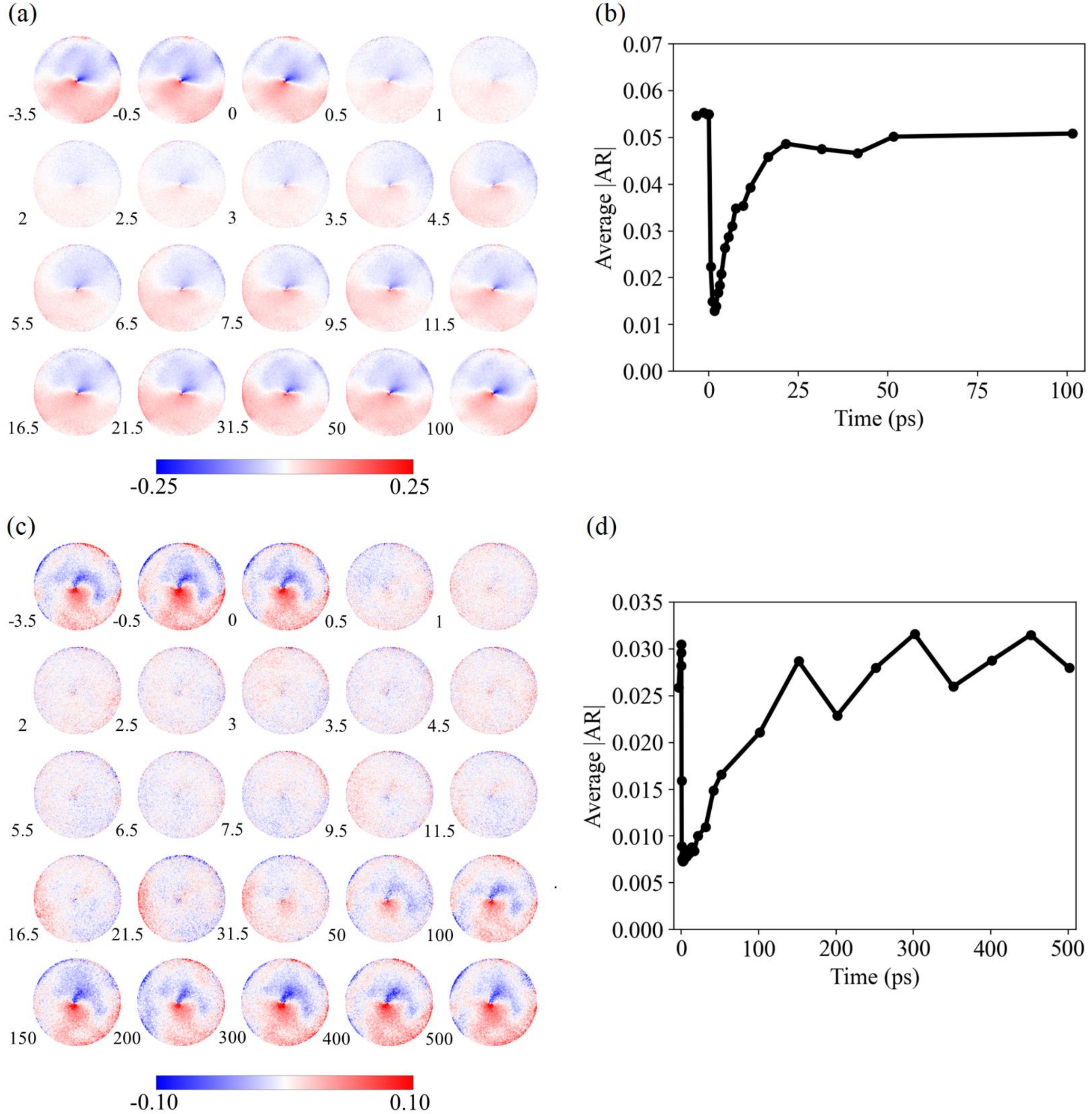

MHDℓ and MHDm for different symmetries

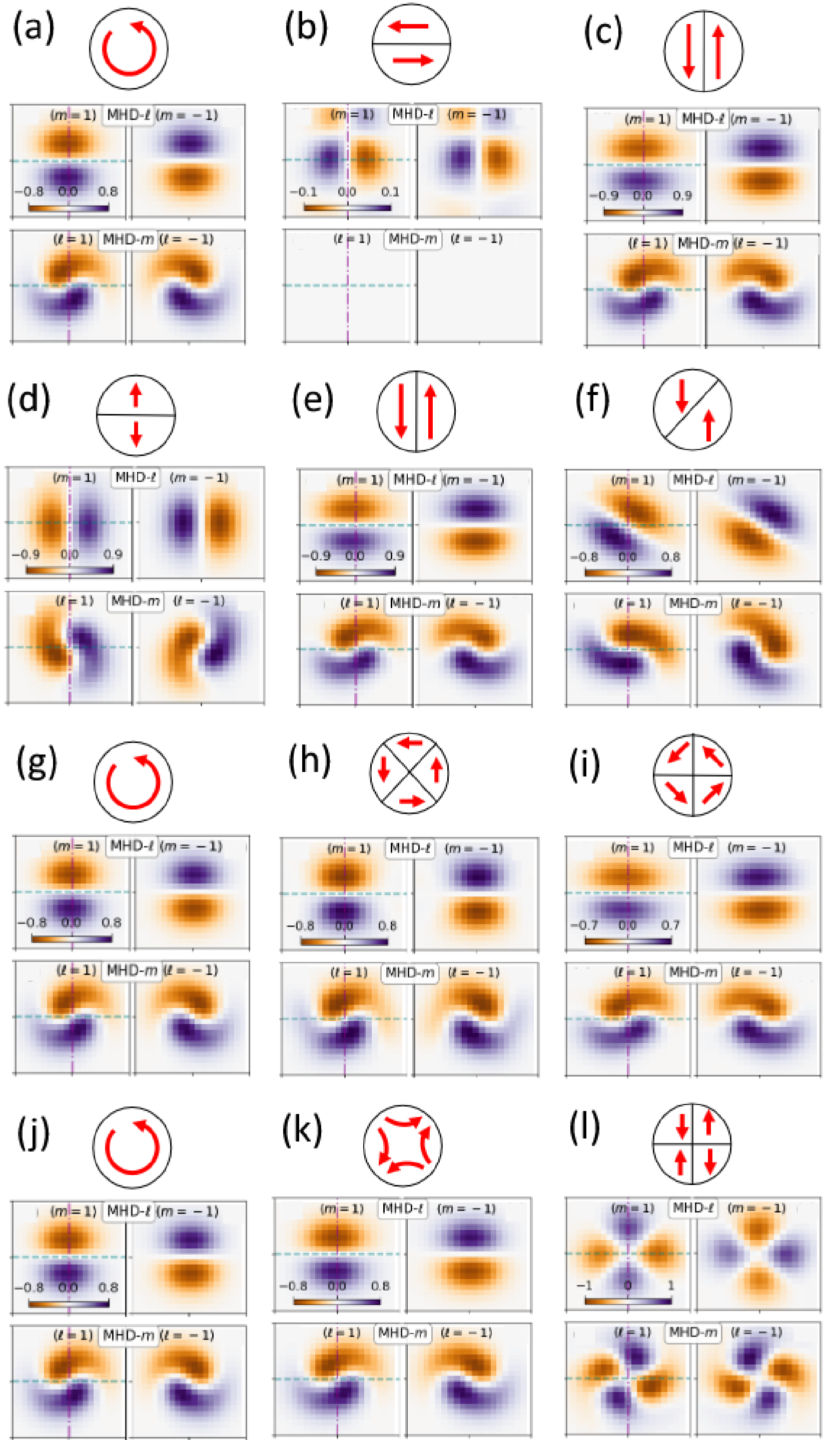

- In our geometry we are sensitive mainly to the my component
- Rotating the domain wall between opposite my components rotates the MHD
- Only small changes in the MHD if we keep the same vorticity
- Vortex and antiortex have same Fourier indices, while other configurations with higher indices give completely different MHD